Evaluating Preferential Recharge in Blue Ridge Aquifer Systems Using Saline Tracers

David F. Rugh

Thesis submitted to the Faculty of Virginia Polytechnic Institute and State University in partial fulfillment for the degree of

MASTER OF SCIENCE

In

GEOSCIENCES

Thomas J. Burbey (Chair)

Madeline Schreiber

Daniel Gallagher

November 28, 2006

Blacksburg, VA

Keywords: Blue Ridge, Groundwater Recharge, Differential Electrical Resistivity Tomography, Borehole Geophysics, Saline Tracers

Evaluating Preferential Recharge in Blue Ridge Aquifer Systems Using Saline Tracers

David F. Rugh

Abstract

Multiple saline tracers were used to explore the role of geologic structure on groundwater recharge at the Fractured Rock Research Site in Floyd County, Virginia. Tracer migration was monitored through soil, saprolite, and fractured crystalline bedrock for a period of 3 months with chemical, physical, and geophysical techniques. Potassium chloride (KCl) and potassium bromide (KBr) tracers were applied at specific locations on the ground surface to directly test flow pathways in a shallow saprolite and deep fractured rock aquifer.

Previous work at the Fractured Rock Research Site have identified an ancient thrust fault complex that is present in the otherwise competent metamorphic bedrock; fracturing along this fault plane has resulted in a highly transmissive aquifer that receives recharge along the vertically oriented portion of the fault zone. A shallow aquifer has been located above the thrust fault aquifer in a heterogeneous saprolite layer that rapidly transmits precipitation to a downgradient spring.

Tracer monitoring was accomplished with differential electrical resistivity, chemical sampling, and physical monitoring of water levels and spring discharge. Tracer concentrations were monitored quantitatively with ion chromatography and qualitatively with differential resistivity surveys. KCl, applied at a concentration of 10,000 mg/L, traveled 160 meters downgradient through the thrust fault aquifer to a spring outlet in 24 days. KBr, applied at a concentration of 5,000 mg/L, traveled 90m downgradient through the saprolite aquifer in 19 days. KCl and KBr were present at the sampled springheads for 30 days and 33 days, respectively. Tracer breakthrough curves indicate diffuse flow through the saprolite aquifer and

fracture flow through the crystalline thrust fault aquifer. Heterogeneities in the saprolite aquifer had a large effect on tracer transport, with breakthrough peaks varying several days over vertical distances of several meters.

Monitoring saline tracer migration through soil, saprolite, and fractured rock provided data on groundwater recharge that would not have been available using other traditional hydrologic methods. Travel times and flowpaths observed during this study support preferential groundwater recharge controlled by geologic structure. Geologic structure, which is not currently considered an important factor in current models of Blue Ridge hydrogeology, should be evaluated on a local or regional scale for any water resources investigation, wellhead protection plan, or groundwater remediation project.

Table of Contents

Table of Figures

Introduction

Investigating possible preferential recharge pathways in heterogeneous fractured rock environments is an essential step in characterizing groundwater flow and recharge processes. Understanding the spatial distribution of groundwater recharge in geologically complex aquifer systems requires extensive long-term hydrologic and geophysical monitoring. This involves periodically measuring the physical, chemical, and electrical attributes of the subsurface. Accurate hydrogeologic models for the Blue Ridge Physiographic province are needed because of an increased demand for sustainable groundwater resources.

The Blue Ridge physiographic province represents a relatively narrow band of complex geology and hydrogeology that stretches from Pennsylvania to Georgia. The Blue Ridge is comprised predominately of igneous and metamorphic rocks that are highly fractured and faulted due to several episodes of shortening and extension throughout the Paleozoic and Mesozoic eras (Dietrich, 1970). Relatively few detailed hydrologic studies have been performed in the Blue Ridge despite the fact that numerous public water supplies exist. During a 2002 drought, existing public water supplies were so depleted that emergency water conservation legislation was enacted and many communities received federal disaster relief (Virginia Department of Environmental Quality, 2003; Weaver, 2005).

A better understanding of groundwater flow is needed for locating new reliable groundwater supplies in the heterogeneous fractured rock aquifers that are commonly found in the Blue Ridge. Investigating groundwater flow with tracer experiments allows in-situ observation and measurement of tracer migration. Many researchers have completed studies using saline tracers in different environments at a wide range of scales (Derby and Knighton, 2001; Vanderborght and Vereecken, 2001; Dyck et al., 2005; Hu and Moran, 2005; Levitt et al.,

2005). Saline tracers are widely used because they behave conservatively in a variety of geologic media, they often occur at low background levels, they are simple to quantify, and they are relatively benign when released into the environment (Levy and Chambers, 1987; Kass, 1998). Saline tracers have also been extensively used in conjunction with electrical resistivity imaging (ER) to monitor fluid movement in a non-invasive nature at a high spatial and temporal resolution in unsaturated soils, saturated fractured rock aquifers, and saturated granular aquifers (Slater et al., 1997; Slater et al., 2000; Singha et al., 2003; Kim et al., 2005; Singha and Gorelick, 2005). Applying tracers to evaluate recharge in the Blue Ridge province has not been previously attempted due to the considerable amount of site-specific knowledge that is necessary for successful monitoring in a highly heterogeneous setting.

This study aims to definitively assess the role of geologic structure on groundwater recharge at the Fractured Rock Research Site (later referred to as the FRRS) in the Blue Ridge province. Previous investigations by Seaton and Burbey (2000; 2002; 2005) , Gentry and Burbey (2004), and White and Burbey (2006 *in press*) provide a wide variety of hydrologic, geologic, and geophysical data used to thoroughly describe this study site. These studies suggest that groundwater recharge in the Blue Ridge is highly correlated with geologic structure; which contradicts the accepted Blue Ridge conceptual model that portrays the regolith as a homogenous unit that transmits recharge in a spatially consistent manner to the underlying fractured bedrock aquifer (Legrand, 2004). Evaluating suspected recharge pathways for this study required applying large volumes of saline tracers at the surface and monitoring plume migration through regolith and fractured rock. Multi-level samplers and a deep well were installed for chemical sampling along the study transect.

Water chemistry was periodically analyzed at multi-level samplers, wells, and springs. ER profiles were gathered periodically along the plume transect to measure changes in the bulk electrical properties of the subsurface. Water levels from pressure transducers and water-level meters were recorded at wells and multilevel samplers in the study area. Physical and electrical monitoring of springs was accomplished with a recording flowmeter and specific conductance electrode. Data gathered during the course of this study are applicable to many sites throughout the Blue Ridge province where thrust faults are present in crystalline rock.

Site Geology and Hydrogeology

The Fractured Rock Research Site is located south of Roanoke, VA near the western margin of the Blue Ridge Physiographic province (Figure 1). This portion of the Blue Ridge is characterized by high relief topography and is underlain by highly metamorphosed sedimentary and igneous rocks. Episodes of compression and extension have resulted in a set of semi-regional northeast-southwest trending thrust faults that are topographically expressed as ridges in the vicinity of the study area (Dietrich, 1970; Seaton and Burbey, 2005).

The research site is underlain by the Ashe Formation which consists of gneisses, mica-schists, and granites. The bedrock at the FRRS is highly fractured and faulted at depth due to ancient reverse faulting (Seaton and Burbey, 2005). Storage within the fractured bedrock is typically limited within the Blue Ridge but can increase significantly near localized fractures (Daniel, 1996; Seaton and Burbey, 2005). Depth to bedrock at the site depends largely on topographic position and ranges from 10 to 20 meters.

Weathering of parent bedrock material has produced regolith of varying thickness and composition throughout the Blue Ridge. Regolith in the Blue Ridge consists of soil and saprolite

that typically retains the structure and foliation of the parent bedrock material (Buol et al., 2000). The type and amount of regolith is controlled by topographic elevation and bedrock weathering susceptibility. Regolith in the Blue Ridge upland can be a major storage reservoir for groundwater (Heath, 1984; Daniel, 1996; Swain et al., 2004). Unweathered resistant bedrock fragments are common in Blue Ridge regolith and their occurrence and size increase with depth.

Blue Ridge aquifer systems include varying amounts of bedrock and regolith. The heterogeneous distribution and anisotropic behavior of these materials results in complex hydrologic systems that are extremely variable on a local scale. The amount of groundwater available in Blue Ridge fractured rock aquifers is locally dependent on fractures, joints, and the hydraulic relationship between the saprolite and bedrock (Swain et al., 2004).

The heterogeneous multi-aquifer system at the FRRS has been extensively investigated by previous researchers who have used a wide variety of hydrogeologic tools to better define the conceptual model of Blue Ridge fractured rock aquifer systems. Initial site characterization was performed by Seaton and Burbey (2000; 2002; 2005) using ER profiling and geophysical borehole logging. During the early phases of the study, 11 wells were drilled to varying depths at different locations throughout the field site (Figure 1). Five wells categorized as “deep” (W2, W3, W7, W9, W10) were cased through the regolith and drilled into the metamorphic fractured bedrock. Six wells categorized as “shallow” (W1, W4, W5, W6, W8, P1) were completed in the saprolite. Hydraulic testing of installed wells, analysis of ER profiles, and chlorofluorocarbon age dating of shallow and deep aquifer waters were used to define a new conceptual model for the Blue Ridge province.

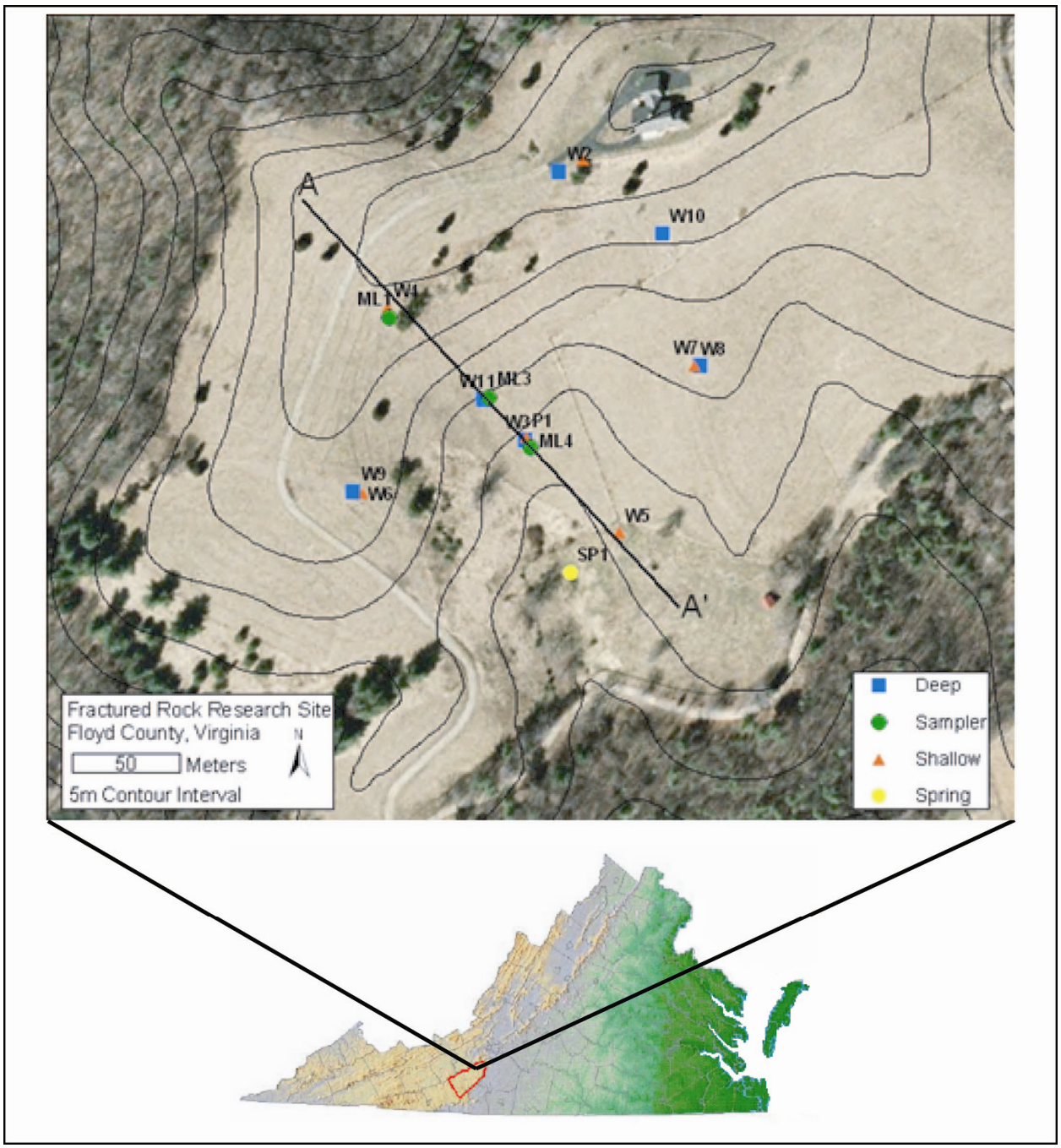

Figure 1: Location map illustrating well (W), multilevel sampler (ML), and spring (SP) locations along the study transect. Line A-A' represents the cross section of the conceptual model and differential resistivity electrode array.

According to previous work conducted by Seaton and Burbey (2000; 2002; 2005), recharge entering the regolith directly above the vertically oriented portion of the ancient thrust fault travels through the unsaturated zone and enters the highly transmissive fractured fault zone aquifer (Figure 2). Recharge entering the regolith elsewhere enters the shallow saprolite aquifer located above a bedrock semi-confining unit and typically travels horizontally along the bedrock surface to local discharge zones such as streams and shallow springs. A localized breach zone permits mixing of shallow and deep groundwater upgradient of a low flow spring found near the southern boundary of the site.

A spring hydrograph study completed by Gentry and Burbey (2004) used hydraulic testing and springflow recording equipment to evaluate the source of shallow spring water. Long term monitoring of water levels, precipitation, and springflow were used to study shallow and deep aquifer discharge to the springhead under different hydraulic conditions. Results indicate that during baseflow conditions, spring (SP1) discharge (Figure 1) consists of 75% deep aquifer water (fault zone) and 25% shallow aquifer water (regolith). During recharge events, elevated springflow is attributed to increased shallow aquifer discharge to the springhead.

Physical monitoring of the unsaturated zone was performed at the FRRS by White and Burbey (2006 *in press*) using time domain reflectometry logging and tensiometers to evaluate recharge mechanisms at the site. Soil moisture and matric potential readings were used to calculate quantitative recharge estimates for several locations along the A-A' transect (Figure 2). The results of this study suggest that the shallow saprolite aquifer and the deep fault plane aquifer exhibit distinct and different recharge processes that reflect the underlying geology.

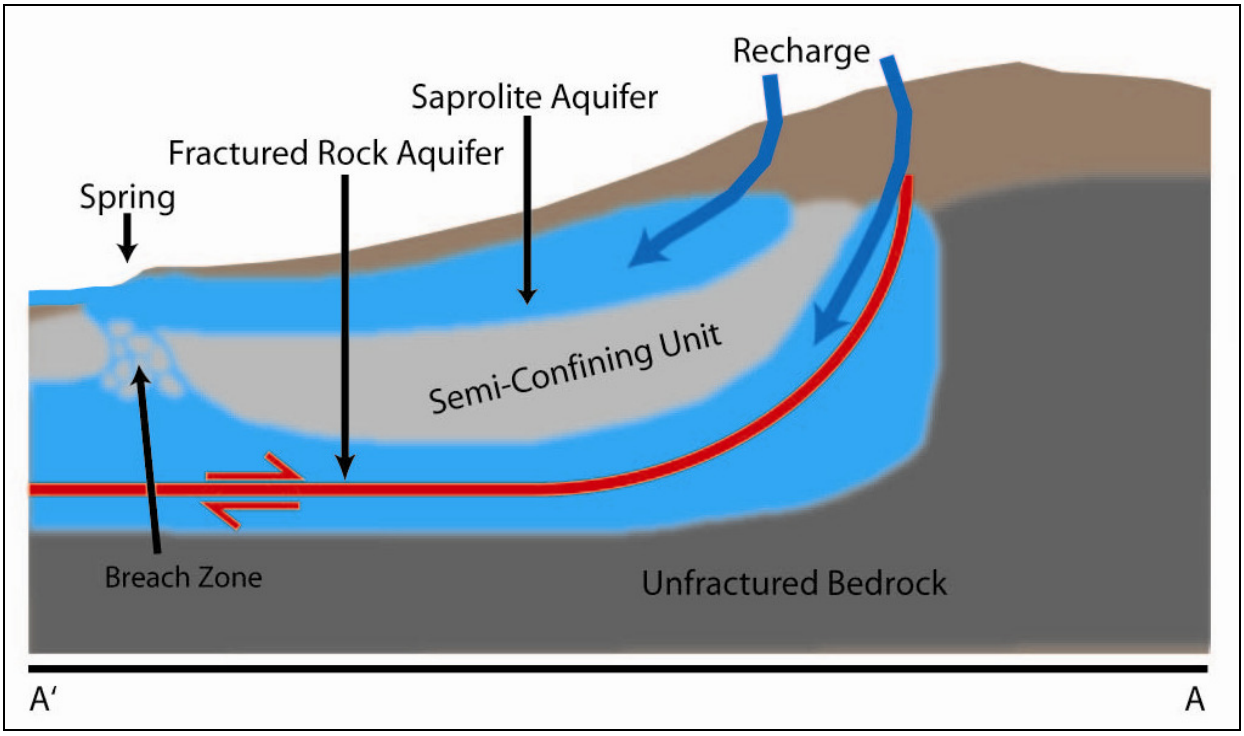

Figure 2. Conceptual cross section of FRRS based on work completed by Seaton and Burbey(2000; 2002; 2005).

Methods and Monitoring

Geophysical Well Logs

Geophysical well logs were used to delineate and characterize fracture zones in deep boreholes used for this study. Existing deep boreholes were previously logged by Seaton and Burbey (2000) during their initial effort to conceptualize the FRRS. This tracer study required a new deep borehole (W11) to be used for further fracture mapping and chemical sampling (Figure 1). Well 11 was logged with a Mount Sopris MGX-II digital logging system that was used to gather spontaneous potential, natural gamma, caliper, 16 inch normal resistivity, 32 inch normal resistivity, 64 inch normal resistivity, and heat pulse flowmeter logs (HPFM).

Interpretation of geophysical logs from W11 yield information that is consistent with the current conceptual model of the FRRS. The gamma, resistivity, and caliper anomaly at ~36 meters is interpreted as the deep thrust fault aquifer (Figure 3). Well 11 was drilled at a unique topographic position; no data pertaining to the depth or transmissivity of the fault zone aquifer were previously available at this intermediate topographic location. A casing leak resulting from a poor seal at the regolith/bedrock interface is visible in the HPFM log at ~21 meters. During HPFM logging during pumping conditions, a large head decline occurred near the casing leak allowing water to enter the borehole from shallow bedrock fractures enters the borehole. This casing leak dominates the HPFM log; other fractures that occur at greater depths appear to produce little water. This effect causes the thrust fault fracture at ~36 meters to appear insignificant even though water levels indicate that this fracture is connected to a portion of the thrust fault aquifer (Figure 4).

An inflatable packer was installed at a depth of 24.4 meters to isolate saprolite aquifer and casing leak water from the deep aquifer. This packer was inflated for the duration of the tracer study. Well 11 was used to monitor tracer migration along the thrust fault.

Well Drilling and Multilevel Sampler Installation

To adequately capture the applied tracers, three multilevel samplers were installed in the saprolite aquifer and one new deep well was packed off to monitor the deep fault-zone aquifer along with W3, W5, and SP1. All holes were completed using air rotary drilling rig. Multilevel samplers ML1, ML3, and ML4 were drilled through the regolith until fractured bedrock was encountered (Figure 1). Deep well W11 was drilled through the fault zone aquifer to a depth of 200' and cased through the regolith. It was discovered after drilling that a poor seal exists between the casing and the bedrock; this prompted the installation of a packer below this interval to ensure that no mixing occurred between the deep and shallow aquifer during the tracer study.

Solinst 3-channel CMT® tubing was installed in ML1, ML3, and ML4 by direct burial using lifts of bentonite chips, sand, and native materials to isolate each sampling port. CMT tubing was chosen because it allows for chemical sampling through minimal purge volumes at three depth zones within a single borehole.

ML1 was drilled into the thrust fault subcrop and has sampling ports at 16m (ML1p1), 17.5m (ML1p2), and 18.5m (ML1p3) below ground surface (Figure 2). ML3 was drilled into the shallow saprolite aquifer and sampling ports were placed at 11.2m (ML3p1), 14.3m (ML3p2), and 17.3m (ML3p3) below ground surface. ML4 was drilled into the shallow saprolite aquifer just upgradient of the breach zone where water from the shallow and deep aquifers mix. ML4 has sampling ports at 10.8m (ML4p1), 9.5m (ML4p2), and 7.6m (ML4p3) below ground surface.

Water Levels and Precipitation Data

Water levels were monitored throughout this investigation using pressure transducers that record hourly measurements. Water levels in the shallow saprolite aquifer were measured with transducers in W4, W5, W6, W7, and P1 (Figure 1). Water levels in the deep fractured rock aquifer were recorded with transducers in W3, W8, W9, and W11 (Figure 1). The data from all transducers were barometrically corrected using data from an onsite barometric pressure logger.

Water levels were measured manually at all multi-level sampling ports during the study. Multi level sampling ports permit hydraulic head measurements and chemical sampling at several depth zones within a single borehole. This study utilized Solinst CMT® tubing that is internally divided into three separate sections for water level measurements and sampling. The size of the Solinst CMT® tubing channel requires the use of a special water level meter that fits in the ~1cm sampling port. These shallow aquifer measurements were made at a minimum twice a week, with increased measurement frequency immediately after precipitation events.

Precipitation was recorded using a self contained battery operated tipping bucket style rain gauge that records the time and date of every 0.01" of precipitation. This logger was periodically downloaded and data were combined into hourly rainfall totals.

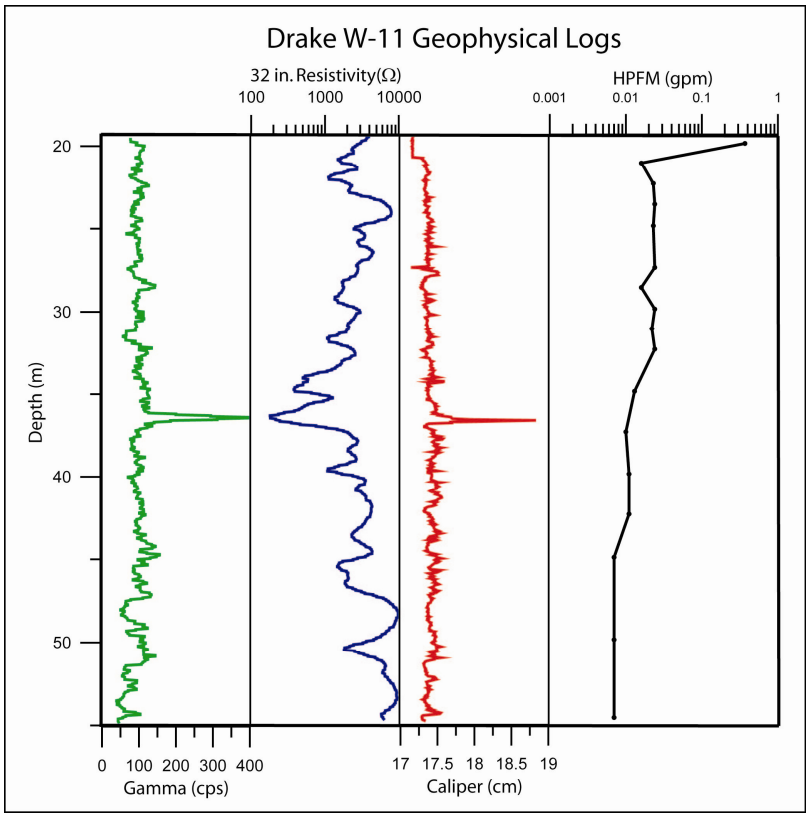

Figure 3: Geophysical logs of W11 show occurrence of a fracture at 36m and inflow of the regolith/bedrock interface at 21m.

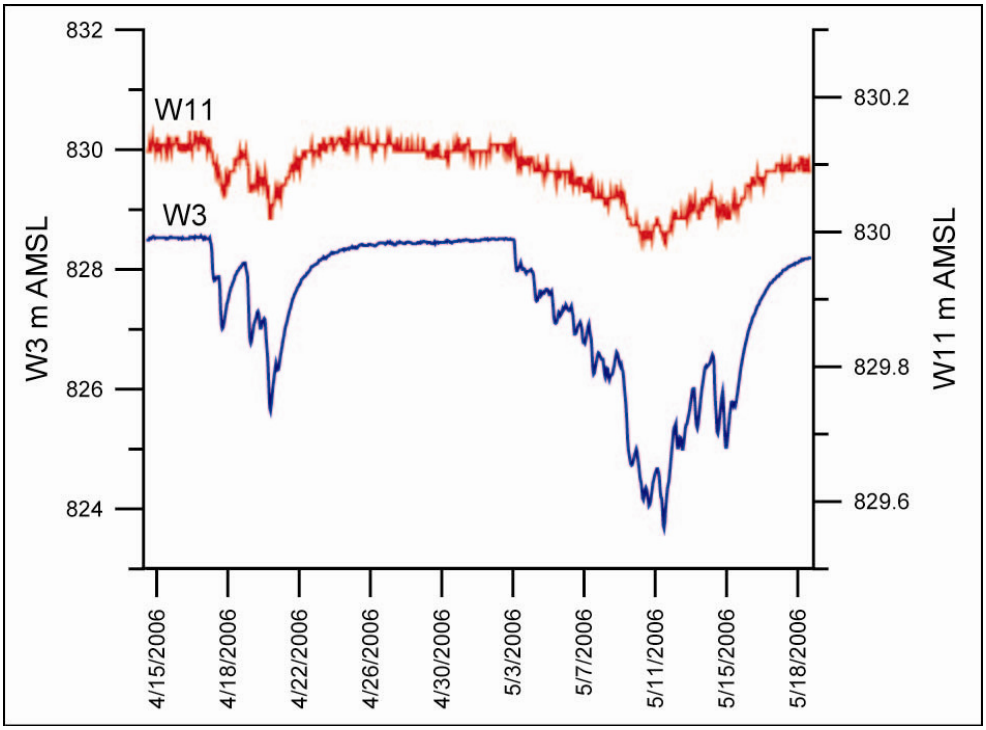

Figure 4: Water level data illustrating hydraulic connection between W3 and W11. The drawdown peaks are a result of fault plane aquifer pumping associated with an infiltration/differential resistivity test run.

Water levels measured during the course of this study support the new Blue Ridge conceptual model proposed by Seaton and Burbey (2000). Water levels of previously installed wells at the FRRS are not discussed because they exhibit behavior that is consistent with previous studies. Water levels from the multilevel samplers installed in the saprolite for this study present new information on water levels and vertical gradients in the shallow aquifer.

ML1, situated near W4 (Figure 1), exhibits a damped response to meteoric recharge due to the depth of the sampling ports below the land surface. Head values monitored from each sampling port consistently differ by less than several centimeters over a vertical distance of 2.5 meters (Figure 5). This small apparent hydraulic gradient is the result of several factors

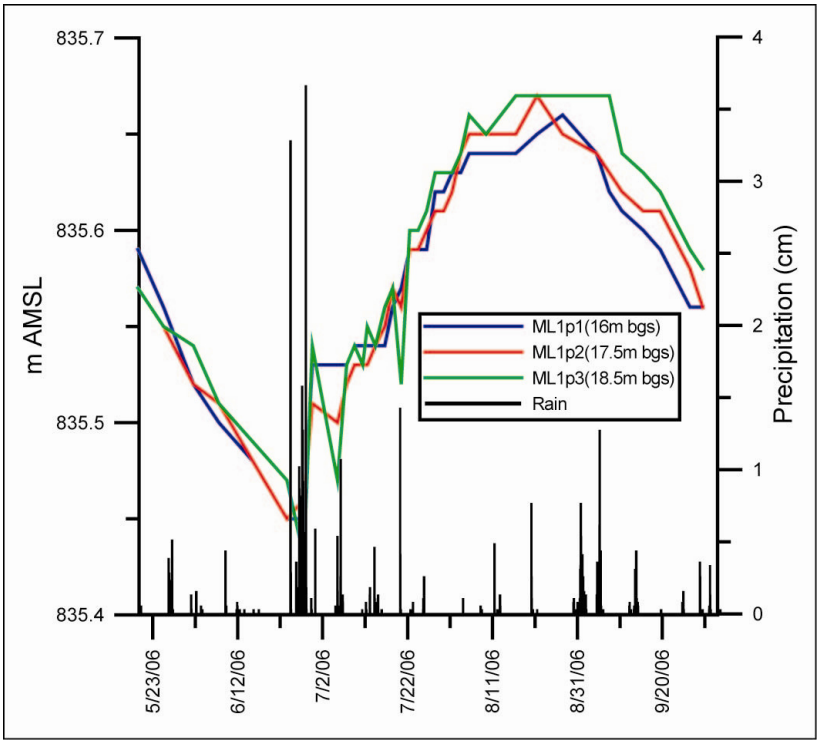

Figure 5:ML1 water levels between 5/19/2006 and 9/29/2006.

including locally homogenous high conductivity saprolite materials, sample port arrangement, and systematic errors from the water level meter. The saprolite encountered during drilling was

a sandy mica-rich soil exhibiting extremely homogenous conditions between the depths of 15m and 19m. Sample port locations were chosen over a vertical distance of 2.5m as a result of the water table depth observed while drilling. Also, the specialty water level meter required for measuring water levels in CMT® tubing is only marked at one meter intervals. The water level meter was used with a meter stick to obtain water levels to the nearest ½ centimeter. Though water level information from ML1 is useful for investigating precipitation response, it is not sufficiently accurate for estimating vertical gradients and flow.

Water levels from ML3 (Figure 1) display a consistent upward hydraulic gradient that supports matric potential measurements repeated by White and Burbey (2006 *in press*). The amplitude of precipitation response from each port is dependent on the depth of the sampling port (Figure 6). ML3p1 responds quickly to a large precipitation event (17cm) between 6/25/2006 and 6/27/2006 and decreases to a new equilibrium water level in a period of eight days. ML3p2 responds to the 6/25/2006 precipitation event as well as a subsequent (4cm) event on 7/5/2006. The second precipitation event only affects water levels at ML3p2.

The hydraulic response of each sampling port can be at least partially attributed to regolith heterogeneity observed during multilevel sampler installation. ML3p3 was completed near the regolith/bedrock interface where large quartz bedrock fragments were encountered. The regolith/bedrock bedrock interface at this location acts as a barrier to vertically infiltrating groundwater and horizontal flow occurs along this boundary. This increased flow explains the large water level response to precipitation observed at ML3p3. Visual analysis of water levels also indicates that the peak water level (831.40 m AMSL) from the 6/25/2006 precipitation event could have occurred between water level measurements. As observed during this study, water level response to precipitation in the shallow aquifer greatly affected tracer movement.

ML4 (Figure 1) was completed upgradient of the breach zone (Figure 2) where the shallow and deep aquifers mix and eventually discharge to the ground surface at SP1. ML4 exhibits an upward vertical hydraulic gradient that is consistent with breach zone aquifer mixing (Figure 7). After a precipitation event on 6/25/2006, the previously upward hydraulic gradient between ML4p1 and ML4p2 reversed for several days. The gradient between ML4p2 and ML4p3 did not change directions during this time. Precipitation loading inputs temporarily reversed the vertical gradient at depths of up to 9.5 m below ground surface allowing for surface infiltration to enter the regolith aquifer.

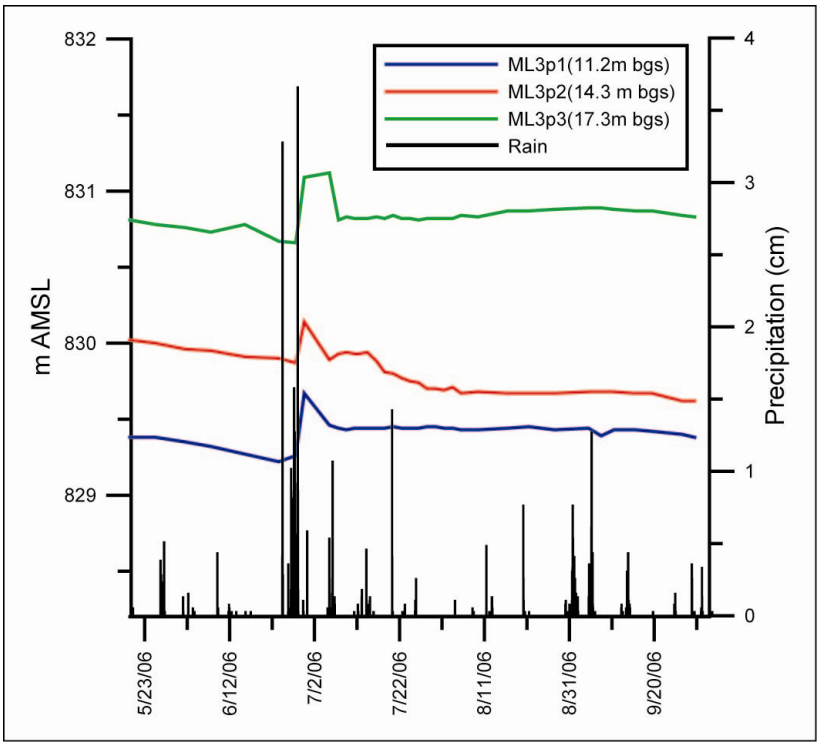

Figure 6: ML3 water levels between 5/19/2006 and 9/29/2006.

ML4 was completed through a sandy interval that was previously interpreted from resistivity surveys completed by Seaton and Burbey (2000). This sandy unit collapsed into the borehole during drilling and made backfilling of the hole difficult and time consuming due to

increased annular volume. The sandy portion of the regolith results in water levels that changed up to 85 cm in two days.

Chemical data gathered during this study suggests that groundwater flow in the saprolite aquifer is highly affected by large precipitation events. Quantifying the water level response to precipitation events is a necessary step in understanding the behavior of the saprolite aquifer. Also, upward gradients consistently measured at ML3 and ML4 would suggest that any tracer present in the thrust fault aquifer could migrate into the saprolite aquifer.

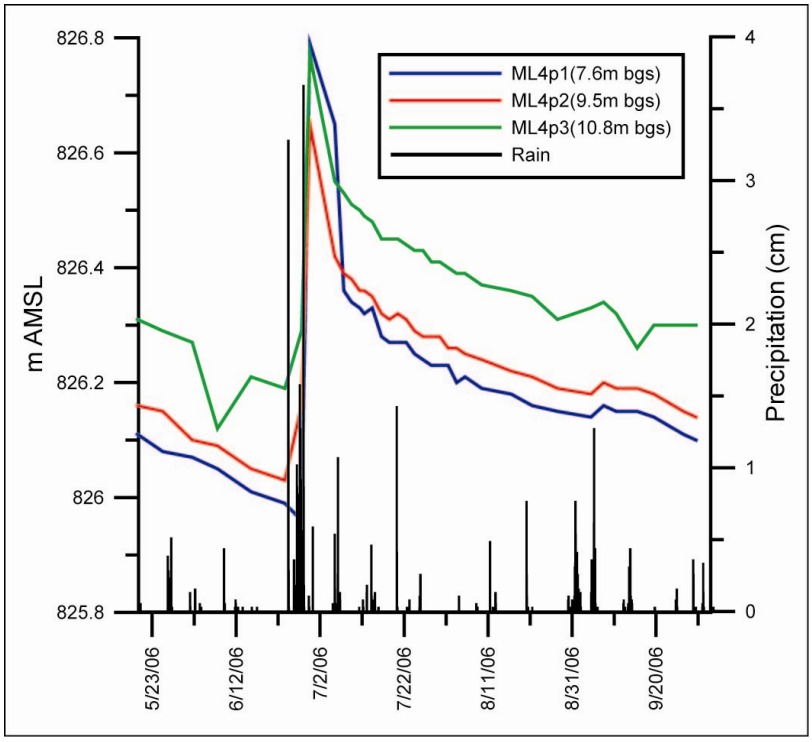

Figure 7: ML4 water levels between 5/19/2006 and 9/29/2006.

Spring Monitoring

SP1 (Figure 1) was monitored between January 2006 and October 2006 in order to correlate water chemistry with springflow. Flow and specific conductance were recorded using a modified version of the low-flow recording system developed by Gentry and Burbey (2004). The recording system consists of readily available electronic components: a paddlewheel flow

sensor, a flow monitoring control box, a specific conductance electrode, a conductance control box, two 12V sealed gel lead-acid batteries, a 4-20 mA data logger, and two 24V solar panels. The data logger recorded flow and conductance data at 10 minute intervals, these data were later combined into hourly values.

This recording system was capable of operating for several weeks without intervention. Because of uncontrollable conditions at the springhead, small amounts of algae occasionally flushed through the recording system and clogged the paddlewheel flow sensor. The paddlewheel sensor and conductance electrode were cleaned during each visit to ensure that accurate flow and conductance data were being measured.

SP1 flow and specific conductance varied little during the monitoring period (Figure 8) except during significant precipitation events (> 5cm). For the 2006 recording period, the average discharge was 5.51 liters per minute (lpm) with a standard deviation of 1.09 lpm and the average specific conductance was 46.94 micro siemens per centimeter (µs/cm) with a standard deviation of 3.02 (µs/cm).

Recent modifications of the springhead performed by the landowner distribute the spring discharge through two separate outlets. SP1, the main outlet, contains approximately ¾ of the discharge and was instrumented with the springflow recording system for this study. SP1B, located several meters downgradient from SP1, contains approximately ¼ of the spring discharge. SP1B was not instrumented, but was chemically sampled with SP1 for laboratory analysis. The springhead modifications resulted in lower springflows that exhibited less variability than those recorded by Gentry and Burbey (2004), which were recorded prior to the modifications.

The specific conductance of SP1 decreases with increased discharge (Figures 8 and 9). Chemical variability at the spring is the result of breach zone groundwater mixing from the shallow and deep aquifers (Figure 2). Deep aquifer groundwater at the FRRS has a significantly higher specific conductance than shallow aquifer water. During the tracer experiment, W3 (deep) had an average specific conductance of 88.9 us/cm and W5 (shallow) had an average conductance of 43.2 us/cm. Deep groundwater discharge to the spring remains consistent through precipitation events while shallow groundwater discharge is heavily influenced by precipitation (Gentry and Burbey, 2004). During elevated springflow conditions, the specific conductance of the springflow decreases as discharge increases (Figure 9). Spring analysis was not a major objective of this study; however, recording apparatus installed for tracer monitoring gathered data that was used for further verification of the FRRS conceptual model.

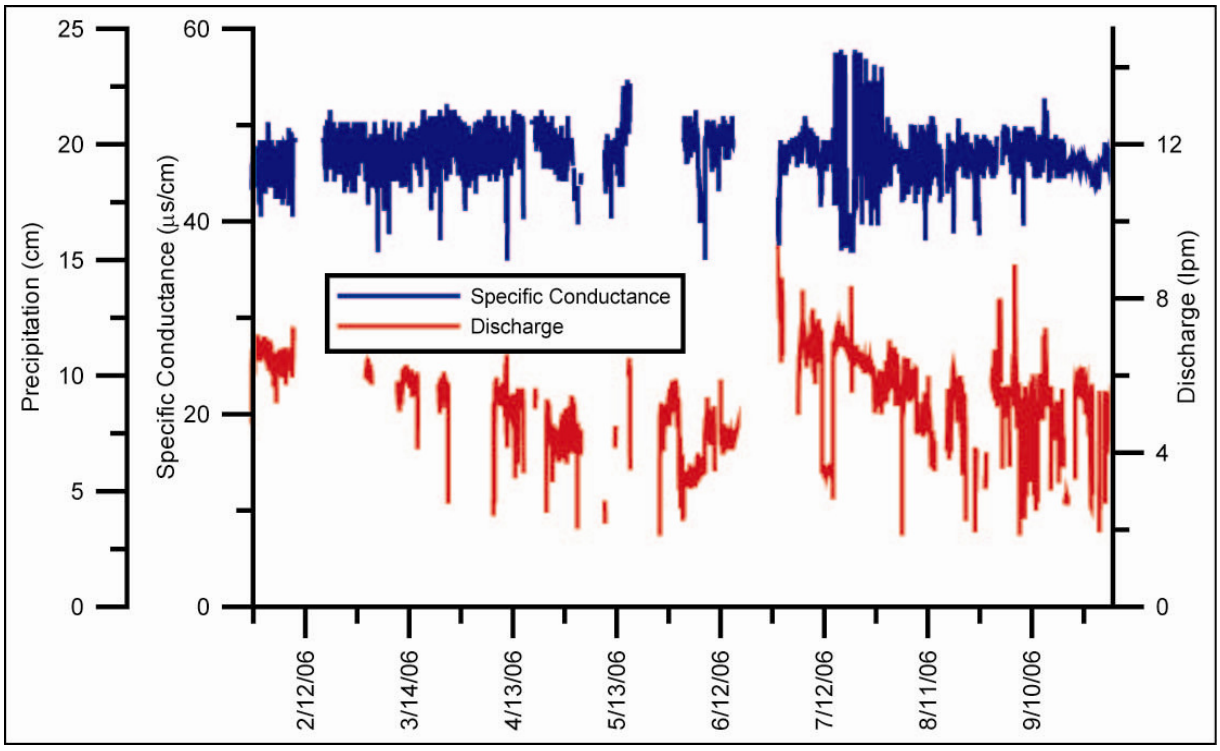

Figure 8: SP1 discharge and specific conductance between 1/27/06 and 10/3/06.

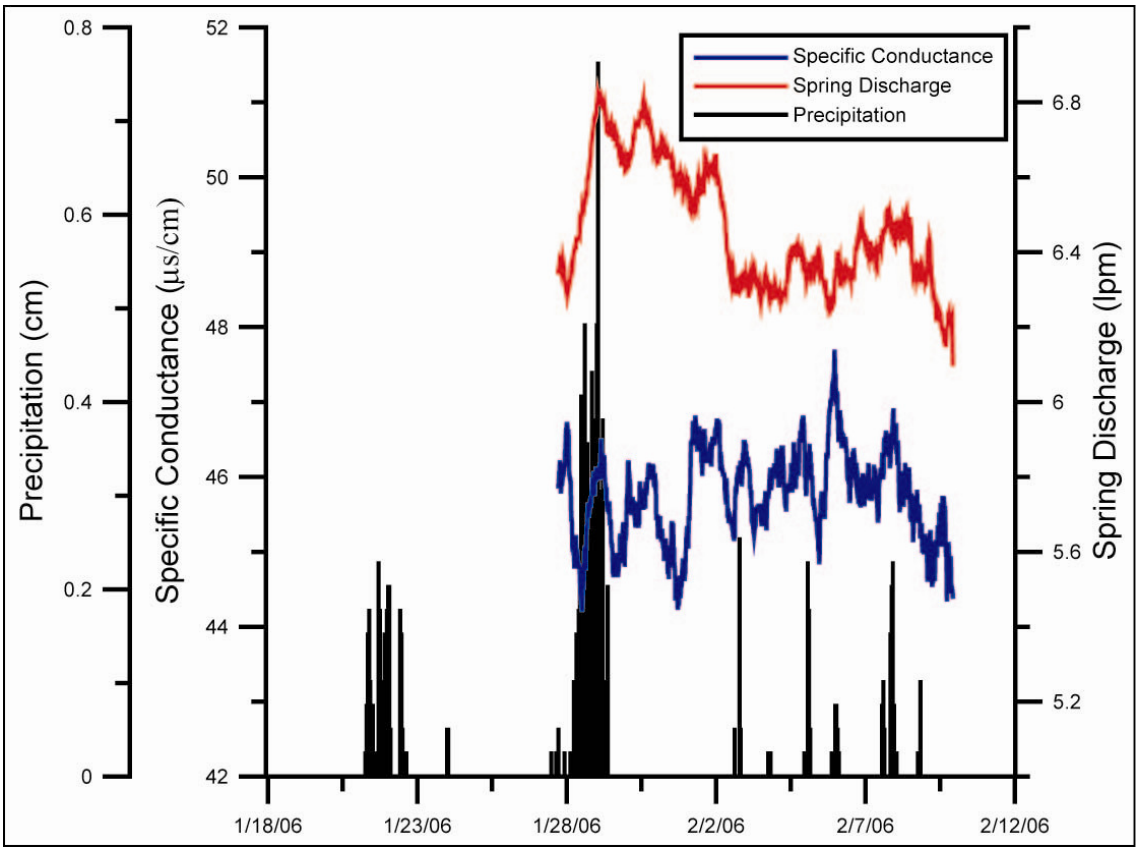

Figure 9: SP1 discharge and specific conductance response to a precipitation event on 1/28/2006.

Soil Sorption Experiments

The saline tracers used during this study must behave conservatively in the geologic media present at the FRRS. KCl and KBr were chosen because they are readily available and simple to quantify using standard ion chromatography. To evaluate the conservative behavior of the Cl^- and Br^- tracers, simple bulk sorption experiments were performed using different soils from the FRRS. Samples were collected with a hand auger near W4 (sample A2), W11 (Sample B2), and ML3 (Sample E1) at three depths ranging from 50cm to 2m (Figure 1). Sorption experiments were conducted by mixing 5g of dry soil and 50 mL of stock solution. Stock solutions contained 0, 10, 50, and 100 mg/L of potassium bromide and potassium chloride. Each

soil solution was adjusted to pH 5 +/- 0.05 with sodium hydroxide or nitric acid. After each soil sample was mixed with each stock solution, the samples were shaken for 48 hours at 25°C on a wrist shaker. Samples were subsequently analyzed using a Dionex DX-120 ion chromatograph with an AS40 autosampler.

Results of the adsorption experiments showed only small amounts of chloride or bromide were adsorbed to the soils (Figure 10). Averaging all depths and sample locations, -0.26% of the applied chloride was lost to sorption (the negative number indicates chloride release from soils) and 4.63 % of applied bromide adsorbed to soil particles.

Sample location A2 (near W4, Figure 1) exhibited the most chloride sorption, with 1.77% of the total applied amount adsorbed at the end of the 48 hour experiment. Locations B2 (near W11) and E1 (near ML3) released chloride throughout the experiment, 1.81% and 0.77% of the total applied mass, respectively. Chloride was later applied in the field as a tracer based on the conservative behavior exhibited in these simple tests.

The largest amount of bromide sorption was observed at sample location E1 (near ML3, Figure 1), with 7.24 % of the total applied bromide adsorbed (Figure 10). Sorption was highest at this location most likely because soils contain a high proportion of clay (Levy and Chambers, 1987; White and Burbey, 2006 *in press*), which provide more possible sorption sites than sand or silt sized particles. Sample location A2 resulted in 4.88% of total applied bromide adsorbed to soil particles. Sample location B2 showed very little sorption over the experiments, 1.88 % of the total applied bromide was adsorbed. During the field experiment, the KBr tracer was applied several meters from soil sample B2 due to minimal amounts of sorption observed in the laboratory.

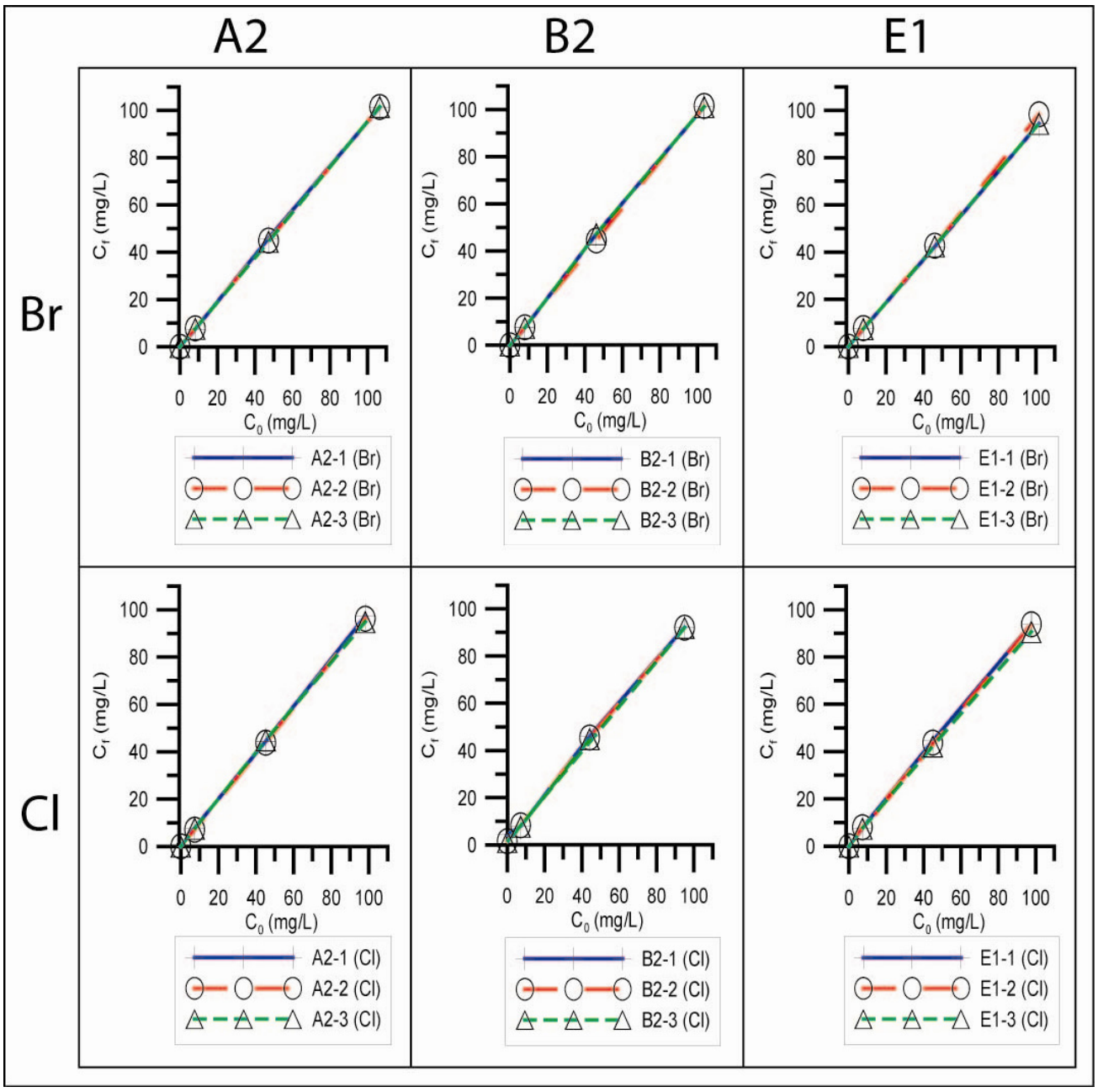

Figure 10: Batch sorption experiments with chloride and bromide solutions using soils from locations A2, B2, and E1. The X axes indicate tracer initial tracer concentration (C_o) and the Y axes indicate the final concentration (C_f) at the end of the 48 hour experiment. A line with a slope of 1 would represent no tracer release or sorption.

Tracer Application

Two separate saline tracers were applied at different locations to evaluate preferential recharge at the FRRS (Figures 11 and 12). The KCl tracer was applied to the soil directly above the suspected thrust fault recharge zone and the KBr was applied at ground surface above the saprolite aquifer over the hanging wall of the thrust fault. Potassium Bromide (KBr) was applied upgradient of W11 and Potassium Chloride (KCl) was applied upgradient of W4. These two tracers were chosen because: (1) they exhibited conservative behavior in Floyd soils, (2) they are not harmful to the environment, (3) they create an electrical signature which allows qualitative monitoring with specific conductance probes and ER surveys, (4) they are present at low background concentrations at the FRRS, and (5) they are easy to quantify in a laboratory setting using ion chromatography.

The tracer concentrations were chosen to minimize density driven flow while still achieving a detectable chemical signature. KCl was applied at a concentration of 10,000 mg/L and KBr was applied at a concentration of 5,000 mg/L. Both tracers were applied using ¾" PVC irrigation piping and a 500 gallon polyethylene water tank.

The tracers were applied at ground surface into 2m x 1m x 2m (l x w x h) pits that were dug with a shovel. Prior to tracer application, a ~500 gallon pulse of freshwater was applied over several days to saturate a small area of the vadose zone (Shapiro, 2005).After this slug of freshwater was applied, the tracer (500 gallon) was continuously released into the pit over the course of several days. An additional ~500 gallon pulse of freshwater was applied after salt infiltration had completed in an effort to advance the tracer through the unsaturated zone.

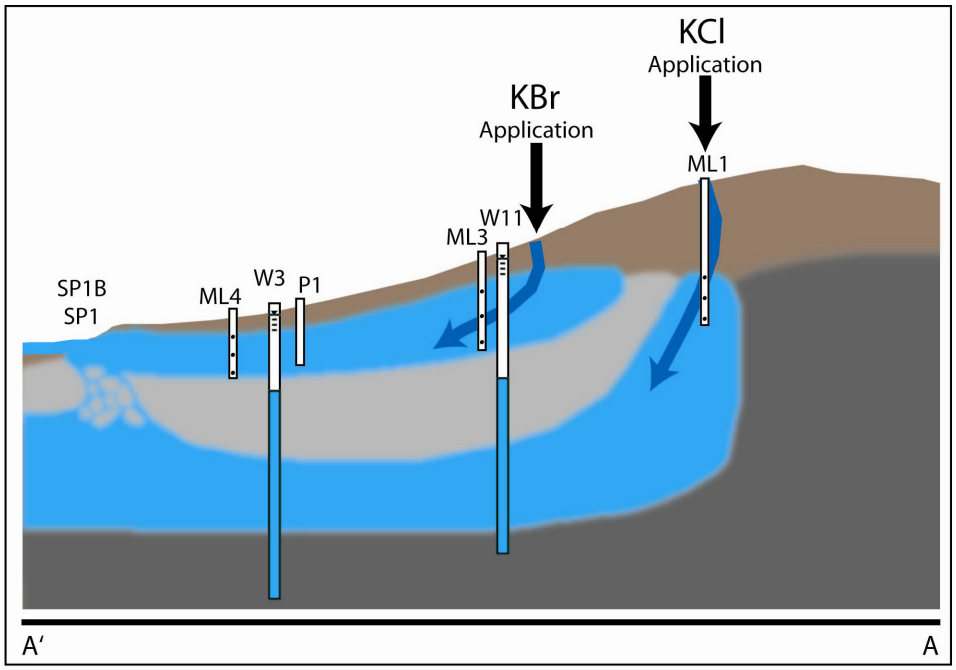

Figure 11: Diagram illustrating multilevel sampler, well, and tracer application locations. Blue lines indicate suspected recharge flowpaths

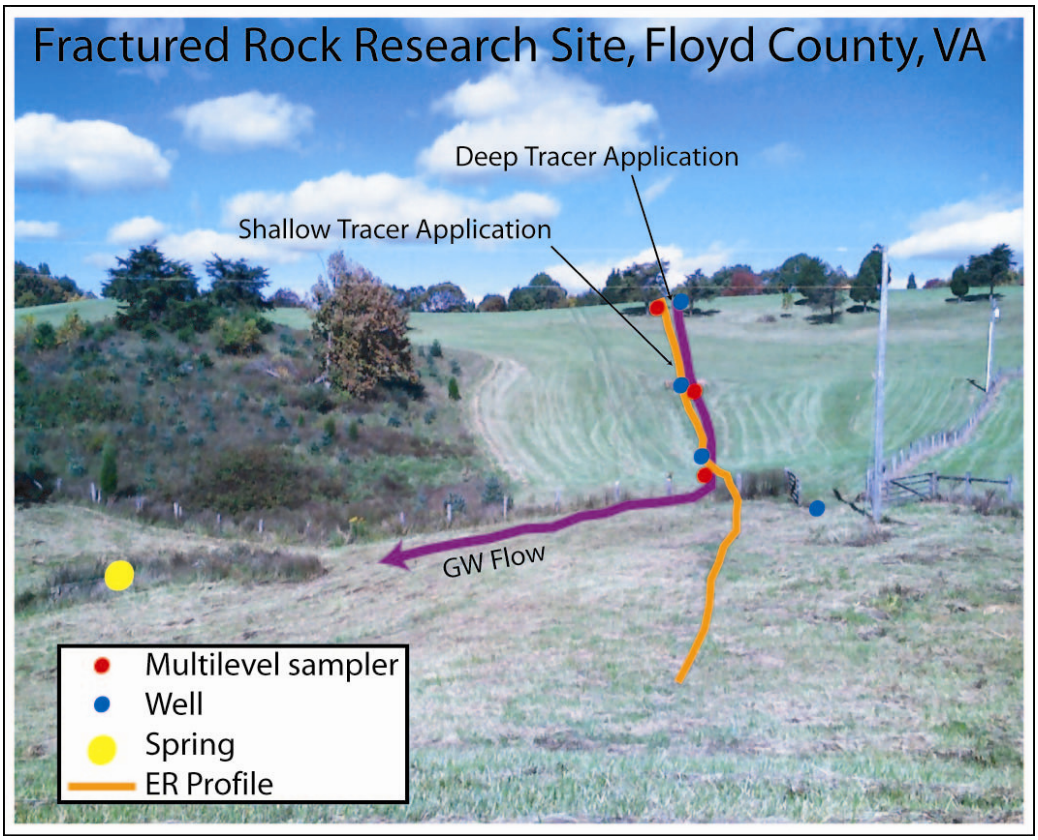

Figure 12: Photograph of the Fractured Rock Research site illustrating the location of the differential resistivity transect, multilevel samplers, wells, tracer application sites, and spring along the study transect.

Application of freshwater and tracer solution was limited by the hydraulic conductivity of the soil, flow rates of ~3 lpm were used to prevent overflowing of the application pits. All water used during tracer application was piped from the farmhouse on the site. The water to the house is supplied by W10, which is completed in the deep aquifer and is located laterally several hundred meters from the study transect. Water level declines in the deep aquifer along the study transect recovered ~24 hours after freshwater application.

Water Chemistry Monitoring

During this tracer investigation, water samples were taken periodically along the study transect at samplers, wells, and the spring. Samples were taken every other day for the first 5 weeks of the study, every third day for weeks five to seven, and twice weekly for the remainder of the study which ended 14 weeks after tracer injection. Specific conductance was monitored during sample collection with a handheld field electrode. All water samples were collected in a 50 mL centrifuge tube and taken to the laboratory for ion chromatography analysis.

Samples collected from multilevel samplers were gathered with a Solinst mini inertial pump. This hand powered pump consists of 2 stainless steel inserts and a stainless steel check ball inserted inside ¼" LDPE tubing. Each multi level sampling port was evacuated prior to conductance measurement and sample collection.

Wells were sampled with a bailer after pumping with a Grundfos Redi flow submersible pump. Wells were not completely evacuated during each sampling event because withdrawing the recommended three wellbore volumes of water could remove significant volumes of Br or Cl tracer from the system. W3, W5, and W11 were sampled weekly during the study to minimize the effects of pumping on the deep aquifer. Wells were pumped according to their casing diameter and depth: ~250 liters was removed from W3, ~100 liters was removed from W5, and

~100 liters was removed from W11. Wells were allowed to recover to pre-pumping levels before conductance measurements were taken and samples were gathered.

Interpretation of quantitative Cl and Br chemical data suggests groundwater flowpaths that are consistent with the conceptual model proposed by Seaton and Burbey (2000). The KCl tracer moves from the application site through the fault zone aquifer to the springhead in approximately one month. Elevated chloride levels are present at SP1 for a period of three weeks (Figure 16). The KBr tracer moves from the application point to the spring outlet in three weeks and is present there for six additional weeks.

Chemical data from ML1 (Figure 1) do not show a statistically significant chloride or bromide breakthrough (Figure 13). ML1 was located several meters off the study transect from the KCL application site. Hill slope limitations on the air rotary drill rig during sampler installation caused the sampler to be installed two meters from its planned location. No KCl tracer breakthrough was observed at ML1 because of the lateral distance between the sampler and the study transect.

Chemical data from ML3 (Figure 1) indicate bromide breakthrough at ports two and three beginning 18 days after tracer application (Figure 14). Elevated levels of chloride were not observed at any ML3 ports during the tracer study indicating that the KCl tracer was present only in the thrust fault aquifer. Bromide was detected at ports ML3p2 and ML3p3 simultaneously, but the concentration at port 2 was higher for the first 10 days then observed at port 3. Ten days after the initial bromide arrival at ML3p2 and ML3p3, bromide concentrations at both ports remained steady at ~1.5 mg/L for 23 days. After three weeks of relatively consistent tracer movement, a precipitation event during day 58 flushed the bromide downgradient and no bromide was measured after 9/4/06 at ML3 for the next 22 days. A very

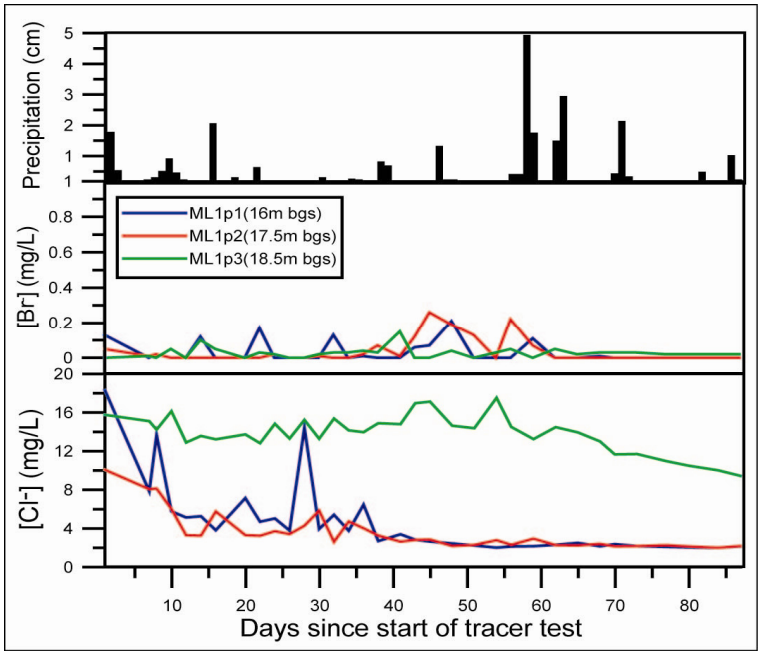

Figure 13: Chloride and bromide concentrations at multilevel sampler 1 (ML1) during the study period. ML1 is located 2 meters laterally from the KCl application site. The KCl tracer was applied at day 1 and the KBr tracer was applied at day 9.

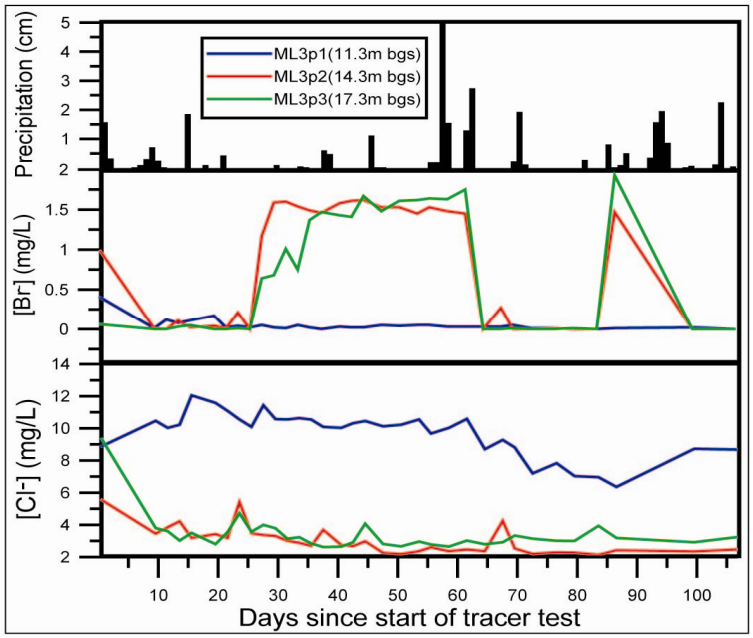

Figure 14: Chloride and bromide concentrations at multilevel sampler 3 (ML3) during the study period. ML3 is located 6m downgradient from the KBr application site. The KCl tracer was applied at day 1 and the KBr tracer was applied at day 9.

short second bromide breakthrough occurred at ports two and three after the 22 day bromide non-detect period. Several samples gathered at ML3 after the second breakthrough did not contain bromide.

Chromatography data from ML4 (Figure 1) indicated bromide breakthrough at all three ports and one elevated chloride peak measured at ML4 port 3 (Figure 15). Bromide was measured at ML4p1 and ML4p3 16 days after bromide application on the surface. Bromide arrived at ML4p2 two days after arrival at ports one and three. Bromide concentrations remained consistent at ports one and two for 37 days after their respective arrivals. Bromide concentrations at port three exhibit a large amount of variability throughout the breakthrough period when compared to all other ports observed during the study. After bromide arrival at port three, concentrations ranged from 0 mg/L to 2.15 mg/L for 14 days. Bromide concentrations at ML4p3 were consistent at ~0.9 mg/L for 23 days after the initial period of variability. Bromide

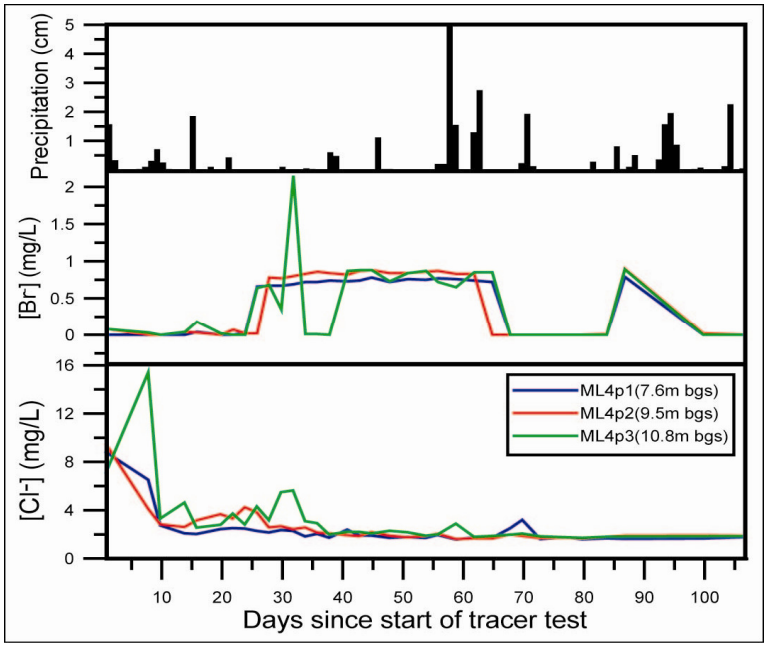

Figure 15: Chloride and bromide concentrations at multilevel sampler 4 (ML4) during the study period. ML4 is located 36 meters downgradient of the KBr application site and 100 meters downgradient from the KCL application site. The KCl tracer was applied at day 1

was not detected at any ML4 ports after day 65 until day 87. A sharp bromide peak appears on day 87 that is coincident with the secondary bromide breakthroughs observed at ML3. This bromide peak consisted of only a single sample from each ML4 sampling port that was sampled near the end of the study when sampling was occurring once per week.

Chemical data from SP1 and SP1B (Figure 1)indicated bromide arrival 19 days after application and increased chloride concentrations 24 days after application (Figure 16). Bromide was detected at SP1 four days before detection at SP1B. Elevated bromide concentrations are observed at SP1 and SP1B for 33 days and 27 days, respectively. A second bromide peak was observed at both spring outlets 23 days after the initial bromide breakthrough ended. This secondary breakthrough is consistent with chemical data measured at ML3 and ML4.

Elevated chloride concentrations were observed for 30 days at both spring outlets. Two distinct chloride peaks were measured on day 24 and day 41. No secondary chloride breakthrough was observed throughout the sample collection period.

Chemical analysis of samples gathered from wells indicated elevated levels of bromide in the fault zone aquifer (Figure 17). Bromide is found at W3, W5, and W11 from day 30 to day 56. A secondary bromide peak consisting of one sample was measured on day 87. W11 consistently had the highest bromide concentrations and W5 consistently had the lowest bromide concentrations. The decline in bromide concentration downgradient suggests a single zone of bromide inflow into the fault zone aquifer; bromide concentrations increased downgradient when the semi-confining unit was leaking in multiple locations. This secondary bromide peak at day 87 coincides with other secondary bromide peaks measured at multilevel samplers and springs.

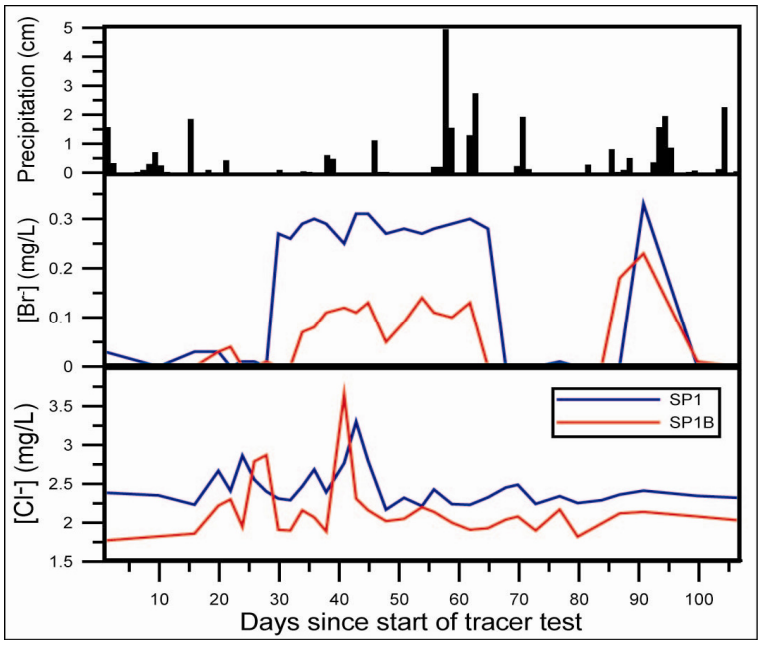

Figure 16: Chloride and bromide concentrations at spring 1 (SP1) and spring 1B (SP1B) during the study period. SP1 and SP1B are located 96m downgradient from the KBr application site and 160 meters downgradient from the KCl application site. The KCl tracer was applied at day 9.

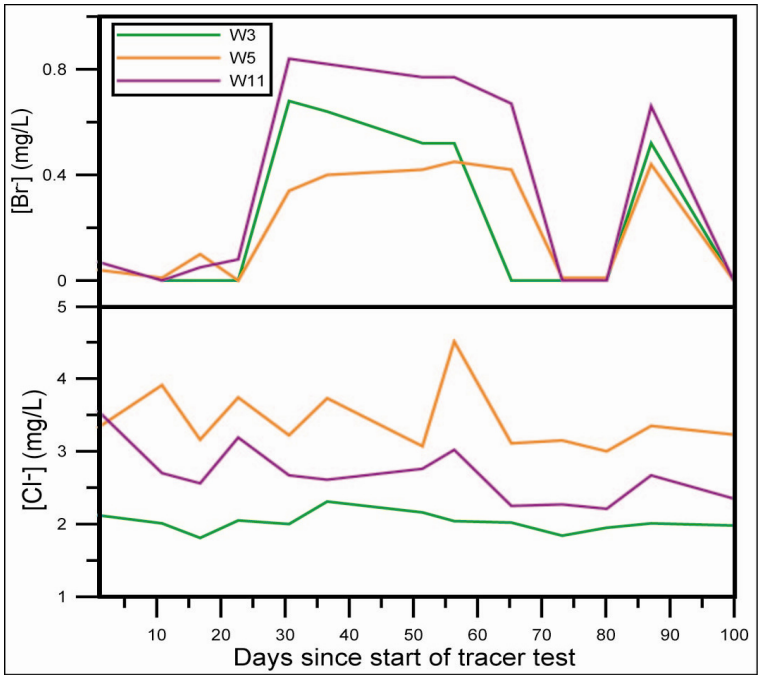

Figure 17: Bromide and chloride concentrations at W3, W5, and W11 during the study period. W11 is located 5 m downgradient from the KBr application area, W5 is 96 m downgradient from the KBr application area, and W3 is 36 m downgradient from the KBr application area.

Differential Electrical Resistivity Surveys

ER surveys were performed periodically throughout the tracer investigation in order to monitor bulk electrical changes in the subsurface due to plume migration. Twenty-five permanent graphite electrodes (Figure 13) were installed at 10m increments along the study transect (Figure 12). Permanent electrodes are preferred for differential surveys because systematic errors due to electrode placement are minimized. Graphite electrodes were chosen over standard steel electrodes because: (1) they exhibit lower contact resistance values than steel, (2) they do not oxidize during long term burial, (3) and voltage potentials do not accumulate at the electrodes.

ER surveys were completed using the graphite electrodes with a 25 electrode Campus Geopulse resistivity unit. A dipole-dipole array consisting of 177 measurements was used to image the FRRS because this array configuration can accommodate the large resistivity contrasts that are present in the Blue Ridge (Seaton and Burbey, 2002).

Resistivity data were inverted using Advanced Geosciences Incorporated Earthimager 2D (AGI, 2006). The smooth model inversion algorithm was used for all data in this study because it is stable, fast, and robust for all types of resistivity data (AGI, 2006). Time lapse inversion uses resistivity datasets from two different times to calculate the spatial change in resistivity over a known amount of time. All time-lapse inversion outputs were saved graphically and in XYZ format for later visual and graphical analysis.

Differential resistivity data collected are consistent with chemical data from multilevel samplers, wells, and springs. The KCl tracer produced a larger resistivity contrast for a longer period of time due to the higher concentration of the chloride tracer solution. The KBr tracer produces a detectable resistivity anomaly of smaller magnitude for a shorter period of time.

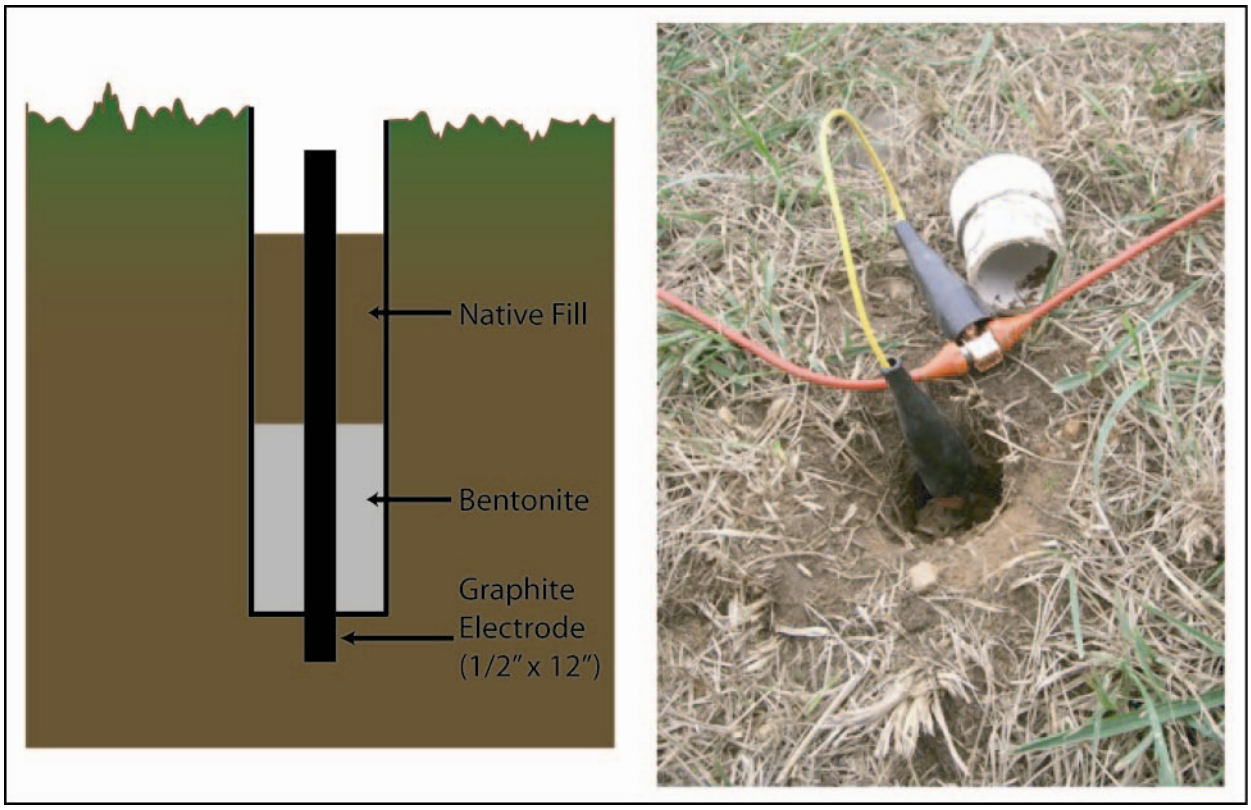

Figure 18: Schematic diagram of graphite electrode installation (left). Picture of electrode attached to resistivity cable with cable lead (right).

The KCl tracer was consistently visible in differential images gathered between the application and the exit from the system at the spring (Figure 16). The high concentration of the chloride tracer allowed the plume to be detected visually with a percent difference scale of +/- 50%. This difference scale was chosen because the KCl plume is easily visible and small-scale variations that are not related to the applied tracer are not considered.

The differential profile collected six days after KCl infiltration reveals rapid vertical movement through unsaturated soil (Figure 19). A very coarse homogeneous sandy soil was noted in this location during drilling. Between day six and day 14, the KCl tracer enters the fault zone aquifer and moves rapidly through the fractured metamorphic bedrock into the deep fault zone aquifer system. The 14 day difference image was gathered when chemical samples from SP1 began to show statistically significant elevated chloride levels. Between day 14 and day 31,

the resistivity difference in the fault zone aquifer increases both in magnitude and physical size. The 31 day resistivity difference image corresponds with the sharp chloride peak visible at SP1 (Figure 19). No plume locations are interpreted in the 71 day difference image because the majority of the KCl had flushed through the system by this time.

No resistivity anomalies have been attributed to KCl presence in the saprolite aquifer, the tracer plume migrated through the thrust fault aquifer under the saprolite aquifer. Chemical data from multilevel samplers are consistent with this interpretation. The slight resistivity difference visible in the 14 day difference image, located near the ground surface at X=140 m, is interpreted to be the downward migration of the KBr tracer in the shallow saprolite.

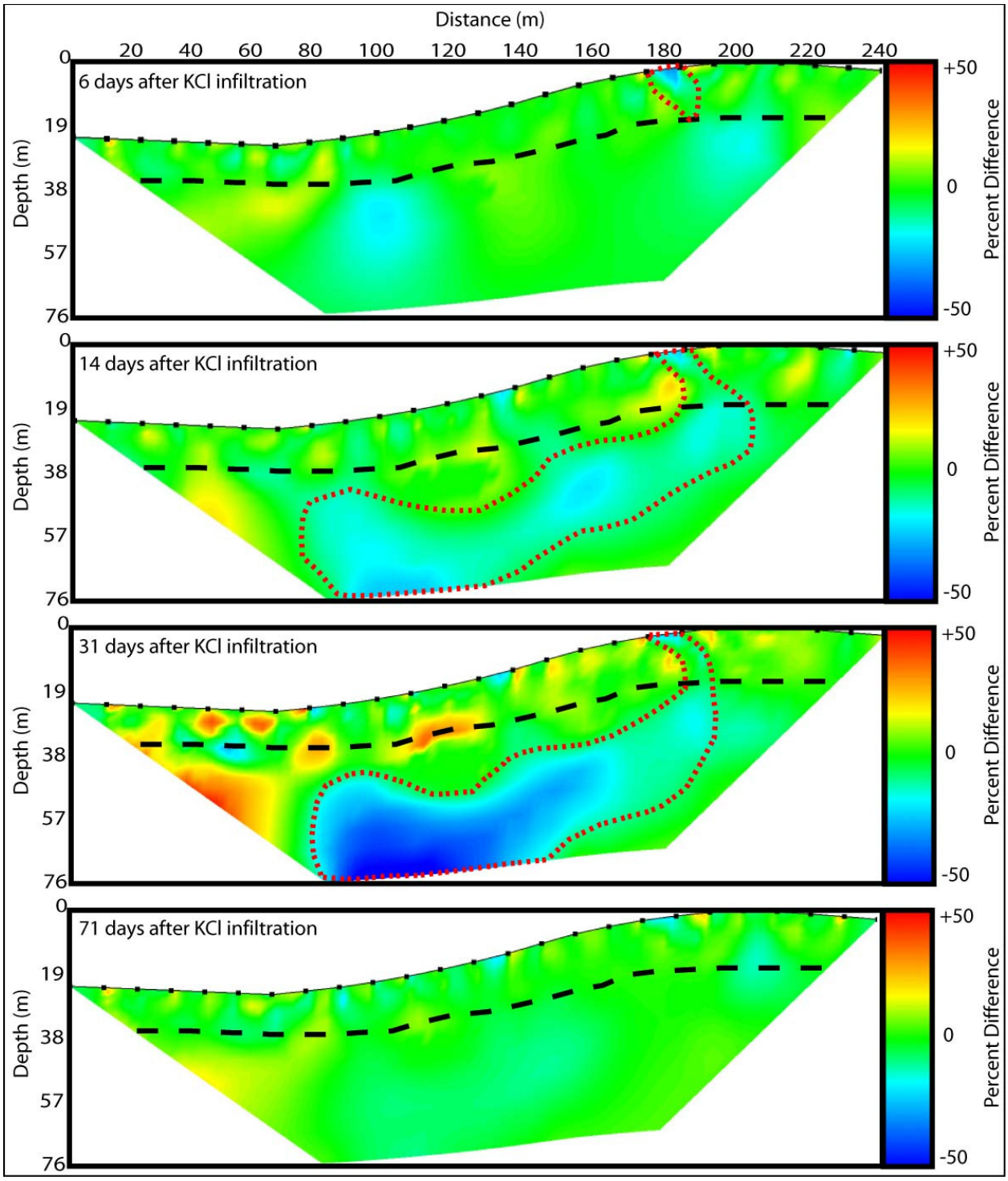

Figure 19: Differential resistivity images showing the movement of the KCl tracer through the fault zone aquifer. The dashed red line indicates the interpreted location of the KCl plume. The dashed black line indicates the bedrock/regolith interface. KCl was applied on the resistivity profile at an x-location of 180 meters. SP1 and SP1b are located laterally off the resistivity section at an x-location of 55 meters.

Discussion

Measurement of water levels, springflows, precipitation, tracer concentrations, and electrical resistivity yielded data that can be used to further constrain the Blue Ridge conceptual model and evaluate the effect of geologic structure on groundwater recharge.

Water levels from multilevel samplers measured throughout this study illustrate the effect of regolith heterogeneity on groundwater flow during infiltration events. Water-level response to major precipitation events (< 5 cm) varied over a vertical distance of 2 meters. Quantifying recharge processes in the Blue Ridge must occur on a local scale and must consider the highly variable hydraulic properties of the regolith.

The upward hydraulic gradient that was consistently measured at ML3 and ML4 was sufficient to cause the KCl tracer from the deep thrust fault aquifer to appear in measurable concentrations at the springhead. The upward gradient would suggest that deep aquifer groundwater flows upward through the semi-confining unit into the saprolite aquifer; no upward fluid migration through the semi-confining unit was observed during this study. Upward chloride migration from the deep aquifer to the spring occurred through the fractured breach zone (Figure 2).

The spring recording system did not provide statistically significant data pertaining to tracer breakthrough as it was intended. Tracer dilution in the groundwater system resulted in low breakthrough concentrations of KCl and KBr that did not affect the specific conductance of the spring discharge. However, all spring data recorded during this study were consistent with the current Floyd conceptual model and data gathered by Gentry and Burbey (2004). Increased springflows are a result of elevated shallow aquifer groundwater discharge to the springhead.

Bromide, which was applied to the shallow saprolite aquifer, entered the deep aquifer as a result of leakage through the W11 wellbore. Bromide concentrations measured at W3, W5, and W11 were relatively consistent throughout the study period, suggesting that bromide was continuously leaking through the W11 casing seal at the regolith/bedrock interface (Figure 21). Bromide was first measured in W11 only two days after it was first measured at ML3p3, suggesting that the bromide tracer must have migrated through W11. Because the bromide solution was applied to the ground surface only 10m upgradient of W11, the tracer solution had to have leaked through W11 around the packer seal or through fractures that are located between W11 and the bromide application site.

Chloride levels measured at ML1, ML3, and ML4 declined throughout the study period due to incomplete screen development after sampler installation (Figure 20). Background concentrations of chloride measured at all multilevel sampling ports were equal to or higher than the chloride concentrations measured after KCl application. Chloride is naturally present at the FRRS due to weathering of micas present in the saprolite; mica was visible in many of the early water samplers gathered from the samplers. The amount of mica in the water samples decreased throughout the study; and therefore the chloride levels also decreased.

Monitoring KCl infiltration and transport with differential electrical resistivity provided qualitative estimates of tracer concentration at a high spatial resolution. Delineating the KBr plume with resistivity did not provide definitive results due to the lower concentration of the applied tracer and the large natural resistivity variations in the shallow saprolite that are not related to tracer movement. Resistivity data proved to be extremely beneficial for monitoring KCl migration in conjunction with chemical sampling. These data proved to be especially important when the KCl plume was located between sampling points.

Average linear velocity estimates calculated from tracer breakthroughs along the study transect can be used to approximate hydraulic parameters for the saprolite aquifer (Figure 20). Heterogeneity in the saprolite aquifer limits the calculation of traveltime data but several breakthrough correlations can be made to extract average linear velocity data. The last positive bromide samples from the first breakthrough at ML3p2 and ML4p1 can be used to calculate an average linear velocity of 30 m/d. Also, correlation of the late time breakthrough peak between ML3p2 and SP1 yields an average linear velocity of 22.5 m/d. These velocity estimates represent the highest conductivity pathways and could vary significantly based on the accuracy of traveltime estimations resulting from the sampling frequency.

Using the chloride peak measured at ML4p3 and the chloride peak measured at SP1B, an average linear velocity of 6m/d is calculated (Figure 20). This velocity differs from those calculated for the saprolite aquifer because groundwater flow in this portion of the groundwater system is dominated by aquifer mixing and preferential flow pathways through breach zone fracturing of the semi confining unit (Figures 2 and 21).

Bromide concentrations measured at the spring were much lower than the actual concentration present in the shallow aquifer before mixing with water from the deep aquifer. Assuming that the spring discharge is 25% shallow groundwater and 75% deep groundwater, all shallow aquifer tracer concentrations are diluted by a factor of four when they exit the springhead.

Analysis of tracer concentrations measured at the spring outlets suggests that outlets SP1 and SP1B contain slightly different proportions of deep and shallow groundwater. SP1 exhibits

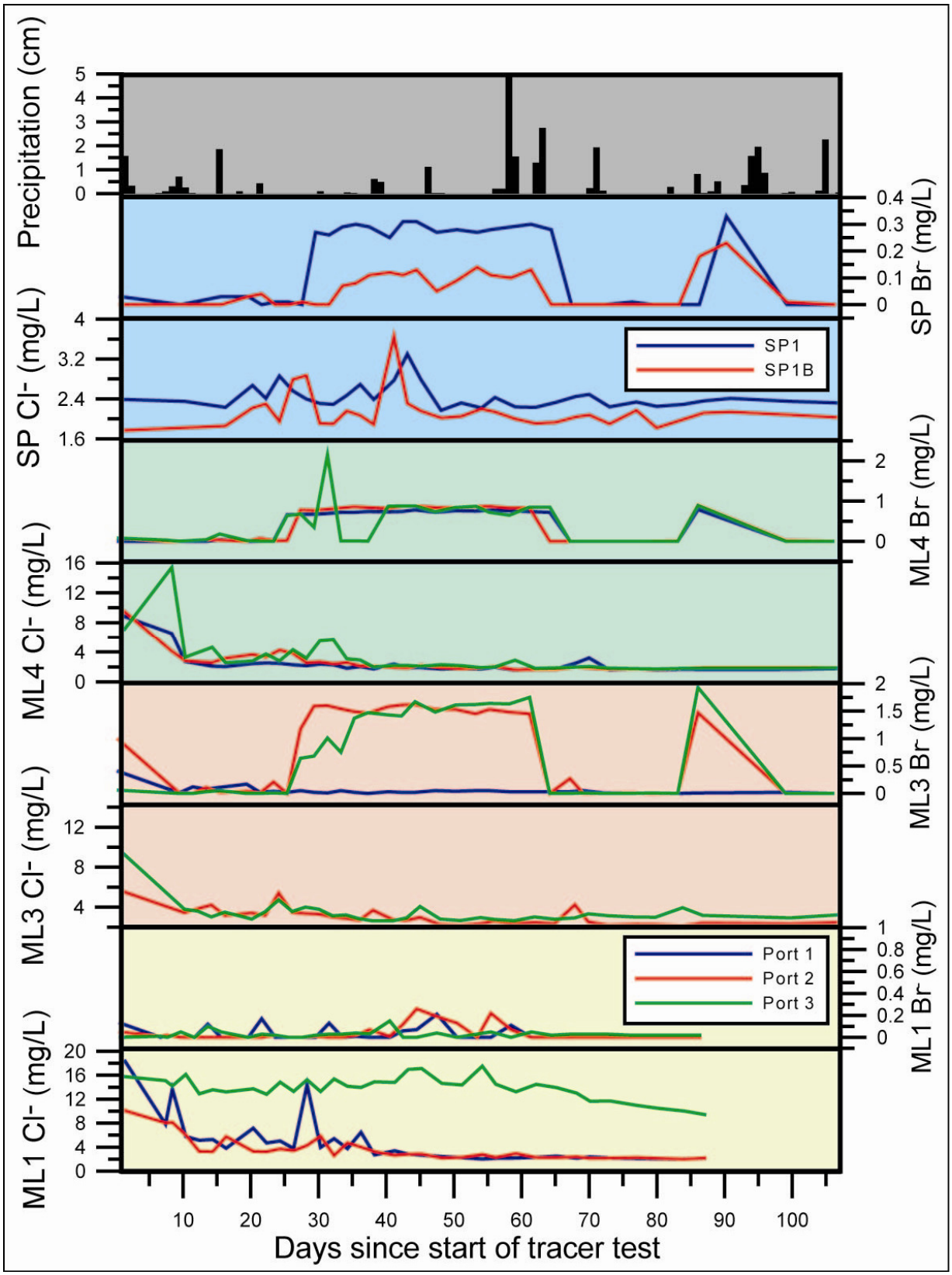

Figure 20: Chloride and Bromide concentrations for all multilevel samplers and spring outlets during the study period. The KCl tracer was applied at day 1 and the KBr tracer was applied at day 9.

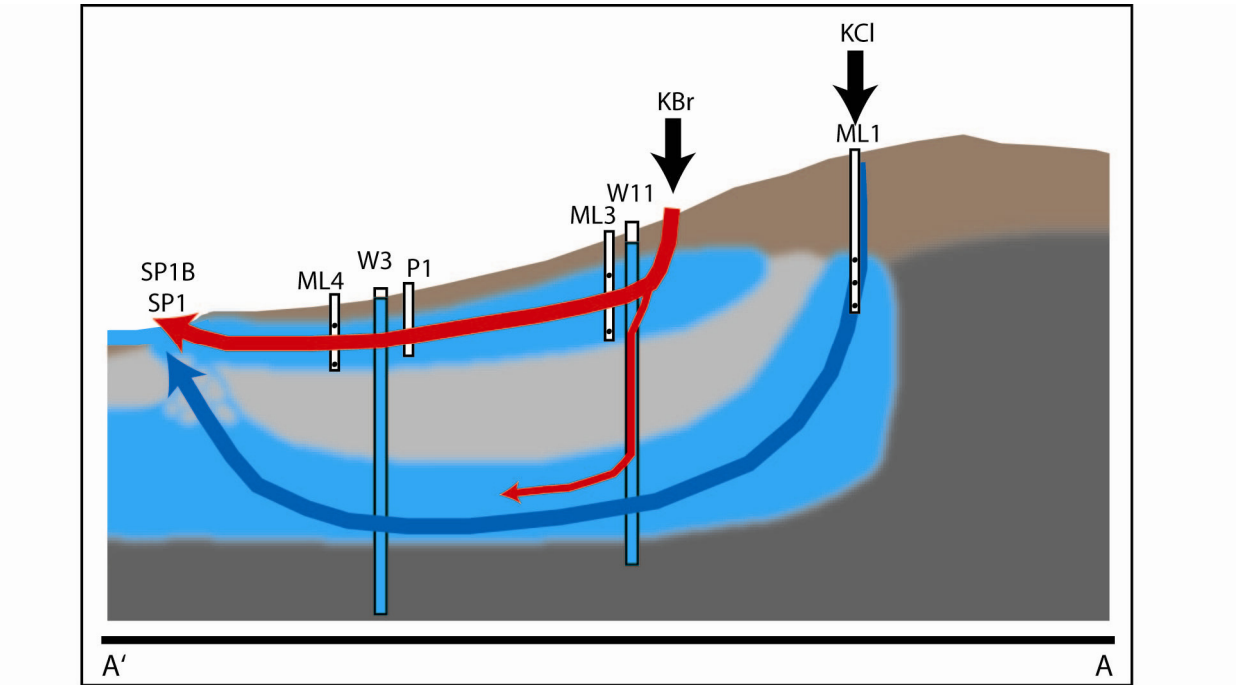

Figure 21: Interpreted tracer flowpaths. Blue line indicates path of KCl tracer and red line indicates path of KBr tracer.

a higher breakthrough for bromide and a less significant bromide peak. SP1B contains higher concentrations of chloride and lower concentrations of bromide. Bromide and chloride breakthroughs are present at each springhead; however, SP1 contains a larger proportion of shallow groundwater compared to SP1B. Differing spring chemistry over a distance of several meters further illustrates the effects of aquifer heterogeneity in the shallow subsurface.

Bromide breakthrough concentrations suggest rapid flow in the saprolite aquifer where tracer migration due to dispersion is minimal when compared to advective transport. Dispersion could extend breakthroughs as the tracer migrated downgradient; this is not observed during the study as bromide was present at ML3, ML4, and SP1 for approximately 30 days. The lack of dispersion observed suggests that fractures could play a significant role in fluid migration in the

saprolite aquifer. Precipitation influences on tracer migration also suggest rapid infiltration and groundwater flow in the saprolite aquifer.

The secondary bromide breakthrough observed throughout the site on day 87 is the product of KBr tracer being released from a low conductivity portion of the regolith. A single source of bromide release could result in nonzero bromide concentrations at several locations along the study transect due to the high average linear velocities in the saprolite aquifer and highly transmissive fractures in the semi-confining unit. Because the secondary bromide breakthrough is also observed in the deep aquifer; the zone of secondary bromide release must have been located between the KBr application zone and W11. It is highly likely that primary and secondary bromide breakthroughs in the deep aquifer are the result of the same fractures or packer leakage. It is also likely that precipitation events could have influenced the timing and magnitude of the second breakthrough peak (Figure 20).

The diffuse nature of groundwater flow observed in the saprolite aquifer is a product of several factors: (1) tracer application over a period of 53 hours, (2) flowpaths of varying length and conductivity due to heterogeneous saprolite material, (3) and sampling frequency. Tracer application over several days was required due to infiltration rates in the application pits. KBr was applied at the maximum flow rate that would not cause the pit to overflow and distribute the tracer solution along the ground surface. The influence of heterogeneous saprolite materials was observed during the study as the KBr tracer migrated through a variety of weathered bedrock in the shallow aquifer. Breakthroughs measured at ML4 suggest lower conductivity material in the vicinity of port 2. Bromide arrives at ML4p2 two days after arrival at ports one and three and disappears at ML4p2 three days before it disappears at ports one and three.

Conclusions

Tracer data gathered during this study suggests that groundwater recharge in the Blue Ridge province is highly controlled by local or semi-regional geologic structure. SE-NW trending ancient thrust faults present in crystalline bedrock can serve as highly productive fractured rock aquifers with a limited recharge area (Figure 22). Saline tracer application above a vertically oriented thrust fault zone verified preferential recharge to a fractured thrust fault aquifer along the fault subcrop. A second tracer application above a saprolite demonstrated high conductivity preferential flow pathways in the regolith near the bedrock surface. Springflow at the FRRS is comprised of shallow and deep groundwater that is not fully mixed upgradient of the spring outlet. Tracer flowpaths and traveltimes were verified with chemical and geophysical methods that produced consistent tracer concentration results.

Saline tracers can be applied to the ground surface under a natural hydraulic gradient to gain information about flow pathways and groundwater velocities. Tracer methods used during this study are applicable for testing flowpaths in a variety of geologic media. As with any tracer investigation, previous knowledge of groundwater flowpaths is required in the planning phases of the experiment. The natural gradient tracer method utilized for this study requires even more background information because constantly changing hydraulic gradients could make plume delineation difficult. This study was successfully completed at the Fractured Rock Research Site in Floyd County, VA because of the access to previous work at the site, and the site topography which drives groundwater towards SP1, a topographically low area representing a local groundwater discharge area.

Though this was a local scale experiment, the findings of this study can be applied to other areas in the Blue Ridge where complex geologic structure creates preferential flow

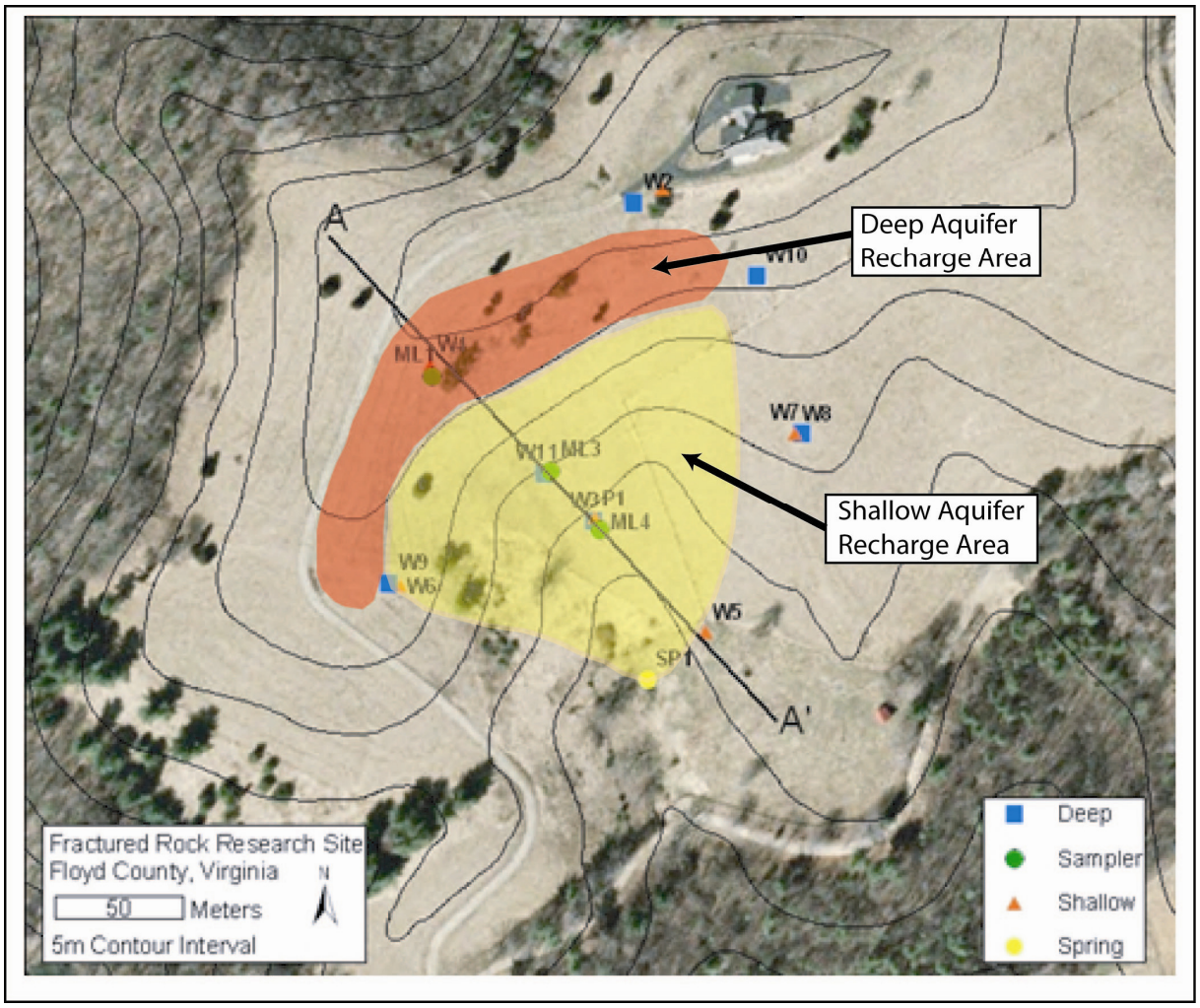

Figure 22: Location map illustrating shallow and deep aquifer interpreted recharge areas.

pathways. Lineament analysis of the Check, VA1:24,000 USGS quadrangle, which includes the study area, reveals a large number of regional scale lineaments with similar orientations to the thrust fault complex investigated in this study (Seaton and Burbey, 2005). The regional geology suggests that complex aquifer systems comparable to the FRRS are common throughout the Blue Ridge; though few detailed hydrologic studies have been completed in the region to validate the presence of fault zone aquifer systems.

Data from this study and previous studies at the FRRS have shown that geologic structure has a significant effect on groundwater recharge. Geologic structure is not considered an important factor in currently accepted conceptual for the Blue Ridge physiographic; despite the extensive faulting that is present throughout the province. Recent studies at the FRRS have resulted in several observations that are not consistent with the current conceptual model: (1) the primary source of groundwater is the fractured thrust fault aquifer, (2) heterogeneity in the saprolite results in preferential flow pathways, (3) separate aquifer systems in the saprolite and fractured rock separated by a relatively unfractured crystalline rock confining unit, (4) preferential recharge along vertically oriented thrust fault zones.

The need for accurate groundwater information in the Blue Ridge province is an ever growing concern as population increases and metropolitan areas in the continue to spread into the surrounding rural areas. Locating sustainable groundwater resources in the Blue Ridge has historically been a difficult task, and it will become increasingly complex as demand increases. Scientists and regulators should consider geologic structures, especially faults, in future groundwater investigations as possible conduits and possibly groundwater reservoirs.

References

AGI (2006). Instruction Manual for EarthImager 2D : Resistivity and IP Inversion Software, Advanced Geosciences Inc.

Buol, S. W., A. Amoozegar, M. J. Vepraskas, G. M. Clark, H. H. Mills and J. S. Kite (2000). "Physical, chemical, and morphological properties of some regoliths in North Carolina." Southeastern Geology **39**: 151-160.

Daniel, C. C. (1996). Groundwater Recharge to the Regolith-Fractured Crystalline Rock Aquifer System, Orange County, North Carolina, USGS Water-Resources Investigations Report 96-4220**:** 67.

Derby, N. E. and R. E. Knighton (2001). "Field-scale preferential transport of water and chloride tracer by depression-focused recharge." Journal of Environmental Quality **30**(1): 194-199.

Dietrich, R. V. (1970). Geology and Virginia. Charlottesville, University Press of Virginia.

Dyck, M. F., R. G. Kachanoski and E. de Jong (2005). "Spatial variability of long-term chloride transport under semiarid conditions; pedon scale." Vadose Zone Journal **4**(4): 915-923.

Gentry, W. M. and T. J. Burbey (2004). "Characterization of Ground Water Flow from Spring Discharge in a Crystalline Rock Environment." Journal of the American Water Resources Association **40**(5): 1205-1217.

Heath, R. C. (1984). Ground-water Reigons of the United States. U. W.-S. P. 2242**:** 78.

Hu, Q. and J. E. Moran (2005). "Simultaneous analyses and applications of multiple fluorobenzoate and halide tracers in hydrologic studies." Hydrological Processes **19**(14): 2671-2687.

Kass, W. (1998). Tracing technique in geohydrology Rotterdam, Balkema.

Kim, J. W., H. Choi and J. Y. Lee (2005). "Characterization of hydrogeologic properties for a multi-layered alluvial aquifer using hydraulic and tracer tests and electrical resistivity survey." Environmental Geology **48**(8): 991-1001.

Legrand, H. E. (2004). A Master Conceptual Model for Hydrogeological Site Characterization in the Piedmont and Mountain Region of North Carolina: A Guidance Manual. North Carolina Department of Environment and Natural Resources**:** 55.

Levitt, D. G., D. L. Newell, W. J. Stone and D. S. Wykoff (2005). "Surface water-groundwater connection at the Los Alamos Canyon weir site; Part 1, Monitoring site installation and tracer tests." Vadose Zone Journal **4**(3): 708-717.

Levy, B. S. and R. M. Chambers (1987). "Bromide as a conservative tracer for soil-water studies." Hydrological Processes **1**(4): 385-389.

Seaton, W. J. and T. J. Burbey (2000). "Aquifer characterization in the Blue Ridge physiographic province using resistivity profiling and borehole geophysics; geologic analysis." Journal of Environmental & Engineering Geophysics **5**(3): 45-58.

Seaton, W. J. and T. J. Burbey (2002). "Evaluation of two-dimensional resistivity methods in a fractured crystalline-rock terrane." Journal of Applied Geophysics **51**(1): 21-41.

Seaton, W. J. and T. J. Burbey (2005). "Influence of ancient thrust faults on the hydrogeology of the blue ridge province." Ground Water **43**(3): 301-313.

Shapiro, A. M. May 11 2005. Personal Communication

Singha, K., A. M. Binley, J. W. Lane, Jr. and S. M. Gorelick (2003). Electrical imaging of tracer migration at the Massachusetts Military Reservation, Cape Cod. Symposium on the

Application of Geophysics to Engineering and Environmental Problems (SAGEEP), San Antionia, Texas, Environmental and Engineering Geophysical Society.

Singha, K. and S. M. Gorelick (2005). "Saline tracer visualized with three-dimensional electrical resistivity tomography; field-scale spatial moment analysis." Water Resources Research **41**(5): W05023.

Slater, L., A. M. Binley, W. Daily and R. Johnson (2000). "Cross-hole electrical imaging of a controlled saline tracer injection." Journal of Applied Geophysics **44**(2-3): 85-102.

Slater, L., A. M. Binley, M. D. Zaidman and L. J. West (1997). "Electrical imaging of saline tracer migration for the investigation of unsaturated zone transport mechanisms." Hydrology and Earth System Sciences **1**(2): 291-302.

Swain, L. A., T. O. Mesko and E. F. Hollyday (2004). Summary of the Hydrogeology of the Valley and Ridge, Blue Ridge, and Piedmont Physiographic Provinces in the Eastern United States. U. P. P. 1422-A**:** 23.

Vanderborght, J. and H. Vereecken (2001). "Analyses of locally measured bromide breakthrough curves from a natural gradient tracer experiment at Krauthausen." Journal of Contaminant Hydrology **48**(1-2): 23-43.

Virginia Department of Environmental Quality (2003). Virginia Drought Assessment and Response Plan**:** 23.

Weaver, J. C. (2005). The drought of 1998–2002 in North Carolina—Precipitation and hydrologic conditions: U.S. Geological Survey Scientific Investigations Report 2005–5053**:** 88

White, B. A. and T. J. Burbey (2006 *in press*). "Structurally Controlled Recharge in the Blue Ridge Province." Hydrogeology Journal.